Accepted Manuscript

Title: *In vitro* blood–brain barrier models for drug research: state-of-the-art and new perspectives on reconstituting these models on artificial basement membrane platforms

Author: Jayati Banerjee Yejiao Shi Helena S. Azevedo

PII: S1359-6446(16)30195-7
DOI: http://dx.doi.org/doi:10.1016/j.drudis.2016.05.020
Reference: DRUDIS 1826

To appear in:

Received date: 21-1-2016
Revised date: 14-5-2016
Accepted date: 31-5-2016

Please cite this article as: Banerjee, J., Shi, Y., Azevedo, H.S.,*In vitro* bloodndashbrain barrier models for drug research: state-of-the-art and new perspectives on reconstituting these models on artificial basement membrane platforms, *Drug Discovery Today* (2016), http://dx.doi.org/10.1016/j.drudis.2016.05.020

Highlights:

- Drug penetration through the BBB is a major challenge for treating CNS diseases
- *In vitro* BBB models are invaluable for evaluating drug transport into the brain
- Benefits and limitations of *in vitro* BBB models in drug research are discussed
- Contribution of extracellular cell culture matrix is generally ignored
- New outlook on reconstituting BBB models on artificial basement membrane platform

In vitro blood–brain barrier models for drug research: state-of-the-art and new perspectives on reconstituting these models on artificial basement membrane platforms

Jayati Banerjee, Yejiao Shi and Helena S. Azevedo*

School of Engineering and Material Science, Institute of Bioengineering, Queen Mary, University of London, Mile End Road, London E1 4NS, UK

*Corresponding author: Azevedo, H.S. (h.azevedo@qmul.ac.uk).

Keywords: Blood–brain barrier; neurovascular unit; *in vitro* models; drug penetration; cell-support materials; artificial basement membrane.

Teaser: Engineering of novel synthetic basement membrane matrices for recreating *in vitro* blood–brain barrier models with enhanced predictability and paving the way towards customisation in drug discovery and development.

In vitro blood–brain barrier (BBB) models are indispensable screening tools for obtaining early information about the brain-penetrating behaviour of promising drug candidates. Until now, *in vitro* BBB models have focused on investigating the interplay among cellular components of neurovascular units and the effect of fluidic sheer stress in sustaining normal BBB phenotype and functions. However, an area that has received less recognition is the role of the noncellular basement membrane (BM) in modulating BBB physiology. This review describes the state-of-the-art on *in vitro* BBB models relevant in drug discovery research and highlights their strengths, weaknesses and the utility potential of some of these models in testing the permeability of nanocarriers as vectors for delivering therapeutics to the brain. Importantly, our review also introduces a new concept of engineering artificial BM platforms for reconstituting BBB models *in vitro*.

Introduction

The blood–brain barrier (BBB) is a dynamic interface that separates circulatory blood from the brain and exercises strong regulatory control over the influx and efflux of molecules between the brain and the bloodstream. Anatomically, the key constituents of the BBB are brain microvascular endothelial cells (BMECs), astrocytic end-feet, pericytes and the noncellular basement membranes (BMs) that surround and separate these key cellular components from one another. These core components, along with neighbouring neurons and microglia, are often singularly appreciated by the term neurovascular unit (NVU; Figure 1) [1]. The BBB endothelial cells (ECs) express tight junction (TJ) proteins that seal the gap between two adjacent ECs, lack fenestrations and possess few pinocytotic vesicles. Thus, the paracellular and transcellular diffusional entry of hydrophilic substances into the brain from the bloodstream are greatly restricted. Moreover, the presence of metabolising enzymes that can hydrolyse a wide array of exogenous compounds, and a well-defined efflux transport system to remove hydrophobic compounds from the cells, further protect the brain from exposure to outside toxins, hydrophobic substances and xenobiotics [2]. Owing to this incredible barrier protection, most of the central nervous system (CNS)-targeted drugs exhibit poor bioavailability because they fail to accumulate in therapeutically relevant concentrations inside the brain parenchyma to exert their desired effects. Alternatively, drugs intended to act peripherally should preferably be prevented from reaching the brain parenchyma to avoid undesirable toxicity. BBB penetration is therefore a crucial aspect that needs to be characterised during different phases of the drug discovery and development programme.

Even though *in vivo* techniques such as brain perfusion are among the most accurate methods for assessing the BBB permeability of potential drug candidates, direct *in vivo* testing is not always the best feasible option during the early phases of drug discovery research when it is often required to screen combinatorial compound libraries. Further, screening of promising hits for toxicity determination is also desirable at an early phase to avoid delays and attrition at later stages [3]. Another important aspect that undermines *in vivo* studies is the differential expression of enzymes, transporters and TJ proteins between humans and other species, such as rodents commonly used in preclinical testing. Quantitative information on the interspecies variation of protein expression at the BBB level can be found in a recent review by Aday and colleagues [4]. Pharmacokinetic evaluations (ADME) are typically performed in rodents and the data are then extrapolated to predict these characteristics in human models. Yet, functional evidence gathered from positron emission tomography images has shown that the human BBB is more permeable to substrates targeting efflux transporter P-glycoprotein (P-gp) than that of rodents [5]. Therefore, it makes more sense to carry out drug permeability and toxicity studies on human *in vitro* models rather than *in vivo* rat models for predicting drug transport across the human BBB more accurately and reducing the attrition rate in the later stages of the drug developmental pipeline. The most simplified approach to reproduce the BBB characteristics *in vitro* is to isolate and culture brain endothelial cells (BECs) in 2D monolayers. However, when BMECs or ECs from brain capillaries (BCECs) are isolated from the NVU and cultured *in vitro* they tend to lose their intrinsic barrier properties and consequently it can be difficult to correlate *in vitro* data with *in vivo* experimental outcomes. The fact that the BBB is a complex dynamic interface, and the crosstalk among each component of the NVU is important for maintaining the integrity of the endothelial barrier, has led researchers to develop transwell co- and tri-culture models to study the influence of astrocytes, pericytes and even neurons in improving the tightness of the BBB *in vitro* [6]. Recent literature has described some innovative models that were generated by the differentiation of ECs from hematopoietic and pluripotent stem cell cultures [7,8]. Newly reported advanced dynamic and microfluidic models mimicking the flow environment that

actually exists *in vivo* have shown considerable, improved barrier tightness especially with human immortalised cell lines when compared with static co-culture models [9,10]. However, these models at their current stage of development are technically demanding and unsuitable for high-throughput studies [11]. Therefore, a continuous ongoing effort is in progress to develop a model that will retain all the major *in vivo* characteristics of the BBB and yet be simple and cost-effective for routine use in high-throughput screens in pharmaceutical research.

A minimalistic design that can be undertaken in this area is to develop a customised *in vitro* model using novel cell culture support materials containing in-built cell signalling epitopes with the ability to instruct cells. Such cell culture platforms can mimic the fundamental functions of the extracellular BMs and, as such, the cells can respond to the cellular cues provided by the matrix. For developing this type of cell culture model, it is important to understand how the BBB BM proteins interact with the NVU and how such interactions affect the BBB phenotype and functions. In this review, we first briefly discuss the molecular nature of the endothelial barrier and the important parameters that one needs to consider in designing cell-based *in vitro* models of the BBB, followed by an overview of the existing *in vitro* cell-culture models. Next, we explore the impact of the BM, as well as cell culture support materials, on the functions of the NVU; finally presenting our ideas from a material research point of view about how we can utilise this knowledge to create novel or improved versions of pre-existing BBB cell culture models *in vitro*.

Molecular insights into barrier tightness

The adhesion of BBB ECs is mediated by TJ and adherens junction (AJ) proteins at the interendothelial cleft, thus sealing the gap between adjacent ECs and thereby regulating the paracellular transport. There are three distinct classes of TJ proteins: (i) the Claudin family comprising Claudin-3, -5 and -12; (ii) TJ-associated MARVEL proteins occludin, MarvelD2 and MarvelD3; and (iii) immunoglobulin superfamily proteins namely junctional adhesion molecules (JAM A, B and C) and EC-selective adhesion molecule (ESAM) [12]. The cytoplasmic C-terminal helical domain of Claudins and occludins is designed to interact with peripheral cytoplasmic adapter proteins such as zonula occludens (ZO-1, ZO-2, ZO-3), cingulin and junction-associated coiled-coil protein (JACOP) [13]. These adapter molecules help to establish a link with the actin cytoskeleton. Besides their significant role in structure formation, the peripheral adapter proteins can play an active part in cell signalling. Claudin-5 is the major isoform found at the interendothelial junctions and a study with Claudin-5-deficient mice has demonstrated size-selective loosening of the BBB allowing diffusion of molecules with molecular weight less than 800 Da [14]. This suggests that Claudin-5 could have a significant role in maintaining BBB integrity. Additionally, Ohtsuki *et al.* have shown that upregulation of Claudin-5 expression in *in vitro* rat BEC cultures can enhance paracellular tightness [15]. Unlike Claudin-5, the exact role of Claudin-3 at the BBB level is still not fully understood. A study has described the degradation of BBB in experimental models of encephalitis or human glioblastoma owing to selective loss of Claudin-3 expression [16]. Liebner *et al.* have reported that the expression of Claudin-3 directly correlates with the Wnt/β catenin signalling pathway promoting the maturation of the BBB during embryonic development [17]. In *in vitro* BBB models, pericytes in co-culture with BECs can mediate the induction of canonical Wnt signalling events for promoting BBB properties [7]. Unlike other members of the Claudin protein family, Claudin-12 lacks N-terminal PDZ domains that are responsible for establishing a link with the cytoplasmic adapter proteins [18]. *In vitro* studies have shown that Claudin-12 can mediate vitamin-D-dependent paracellular calcium absorption [19]. A study aiming to characterise the localisation of Claudin-12 in human hCMEC/D3 cell lines concluded that it is not localised at the TJ of the primary brain endothelium, even though it is expressed by primary and transformed brain endothelium [20]. By

contrast, its expression and localisation at the TJ was prominent during brain development in a murine model [16]. It is possible that *in vitro* localisation of Claudin-12 at the TJ might need specific cues from astrocytes or pericytes because, in the aforementioned study conducted with hCMEC/D3 cells, co-culture conditions were not used because the cells were unresponsive to astrocyte conditioning. Furthermore, a literature report has also indicated that the ratio of Claudin-5 to Claudin-12 might be significant for TJ establishment; in rats, the expression of Claudin-5 is 751 times higher than that of Claudin-12 [15].

The key constituents of the AJ are vascular endothelial cadherin (VE-cadherin) and platelet endothelial cell adhesion molecule (PECAM). The linker molecules that link AJ proteins to the actin cytoskeleton are the catenins (α, β, γ and p120) [13]. Unlike epithelial cells, where AJ and TJ are distinctly separate, in ECs the AJ and TJ are structurally and functionally related. For instance, it has been reported that VE-cadherin can upregulate the gene encoding expression of TJ protein Claudin-5 [21]. From the perspective of *in vitro* model development with strong barrier characteristics, it is essential to prioritise factors that can significantly upregulate the expressions of Claudin-5, occludin, ZOs and AJ protein VE-cadherin. Antibodies to Claudin-5, occludin and ZO-1 are commonly used as qualitative markers to identify the expression of these proteins in *in vitro* monolayer cultures of BBB ECs.

Quantitative and qualitative parameters defining BBB

A perfect cell culture model would ideally mirror BBB phenotypes and functions that exist *in vivo*, however such an ideal situation is difficult to realise especially with systems as complex as the BBB. In principle, an ideal BBB model for drug testing needs to incorporate the following features: expression and localisation of endothelial TJ and AJ proteins, selective permeability to molecules based on their oil–water partition coefficient and molecular weight, selective and asymmetric permeability to physiologically relevant ions, low fluid phase activity, expression of relevant nutrient and efflux transporters, receptors and drug-metabolising enzymes, easy culture conditions and low cost [22]. In *in vitro* cell models, the barrier tightness of the BEC monolayers is quantitatively assessed by measuring transendothelial electrical resistance (TEER), which measures the resistance towards diffusion of Na^+ and Cl^- ions. This value provides a rough estimate of barrier tightness because actual TEER is unmeasurable for brain capillaries *in vivo*. In adult rat brain parenchymal vessels, an approximate electrical resistance as high as 8000 $\Omega \cdot cm^2$ has been estimated on the basis of combined permeability measurements of three radioisotopic ions (sodium, potassium and chloride) and the TEER in brain arterial vessels is around 1200 $\Omega \cdot cm^2$ [23,24]. Based on these data, it is safe to estimate a TEER of more than 1000 $\Omega \cdot cm^2$ in the mammalian BBB, including that of human. Even though a minimum TEER range from 150 to 200 $\Omega \cdot cm^2$ is sufficient to carry out drug permeability studies [25], higher TEER is more likely to reflect a strong TJ with enhanced resistance to paracellular diffusion; therefore, achieving superior TEER is the fundamental criteria for evaluating the quality of BBB models. However, it is prudent to exercise caution when comparing the effectiveness of different BBB models solely on the basis of TEER because TEER depends largely on the experimental procedures adopted [26]. For example, TEER value depends on the measuring equipment – TEER measured by two different types of instruments [traditional voltohmmeter type chopstick electrodes (EVOM) vs modern cellZscope® system] would be different, and therefore is not recommended for comparison. Again, measurement using the chopstick method might not accurately reflect the true value of TEER because measurement varies with the position and angle of the electrodes. Finally, in addition to TJ protein composition, size of the compound of interest can also affect TEER. In transwell cultures, ECs are seeded on a polyethylene or polycarbonate filter insert coated with cell-support materials. The filter inserts divide the transwell chamber into two distinct compartments – the apical or upper compartment representing the blood side and the lower

or basolateral compartment representing the brain parenchyma. The TEER value of the confluent endothelial monolayer is obtained by inserting two electrodes, one on each compartment, separated by the semipermeable filter insert (Figure 2). If the TEER for controls, as shown in Figure 2bi and 2ci, is not measured and subtracted properly then it can mislead the interpretation of results regarding the actual contribution of the ECs towards TEER for that particular model.

Interestingly, it has been found that TEER varies depending on the pore size, choice of filter material and seeding density. Polyethylene terepthalate (PET) filters can impart better barrier properties than polycarbonate filters, whereas membrane pore size of 0.4 µm has shown the highest TEER value in comparison with pore sizes of 1, 3 and 8 µm in murine *in vitro* BBB models [27]. A paper published very recently by Vandenhaute *et al*. helps in explaining this lowering of TEER with increasing filter pore size [28]. In their quest to optimise an *in vitro* BBB model that would allow migration of metastatic cancer cells across the seeded endothelial monolayer, Vandenhaute and colleagues observed a second layer of ECs on the lower opposite side of the filter with a pore size of 3 µm. They reasoned that ECs from the seeded monolayer at the top of the filter could cross the filter insert because of the larger pore size and colonise on the bottom face of the filter. Because of this double layer formation, the model deviates from the actual monolayer structure that persists *in vivo*. The polarity of the barrier system might even be destroyed because of the presence of this second layer. Consequently, the authors reported a decrease in permeability coefficient, and possibly this led to the decrease in TEER observed. A minimal optimal seeding density of 4×10^5 cells·cm^{-2} has also been found to be crucial for increasing TEER [29].

In addition to electrical resistance, the paracellular transport capacity can be determined by measuring permeability of tracer compounds, such as sodium fluorescein (NaF), lucifer yellow (LY), fluorescein isothiocyanate (FITC)-labelled dextrans, FITC-inulin, FITC-bovine serum albumin, sucrose and mannitol. The marker compounds cannot be potential ligands for membrane receptors and efflux transporters or a substrate for BBB-metabolising enzymes. The endothelial permeability coefficient (P_e) of sucrose in *in vivo* rat models can be as low as 0.03×10^{-6} cm·s^{-1} [30]. Usually TEER and P_e have direct correlation for small hydrophilic molecules, however paracellular permeability is largely dependent on the molecular weight and charge of the molecule and as such cannot be extrapolated for just any solute. Therefore, to get a more realistic assessment of barrier permeability, it is advisable to measure permeability of tracers with different molecular weights [e.g., 0.18 kDa mannitol, 0.342 kDa sucrose, 0.45 kDa LY, 3kDa Texas Red (TXR)-dextran, 20 kDa tetramethylrhodamine (TMR)-dextran and 70 kDa FITC dextran] [31]. Moreover, the correlation between TEER and permeability measurement is also influenced by different experimental protocols, hence TEER and paracellular permeability data should be considered in analysing the quality of the model in terms of barrier permeability [26].

The brain EC membranes express a broad range of ATP-binding cassette (ABC) transporters that prevent many hydrophobic drugs from entering the brain and also excrete harmful metabolic waste out of the brain. In humans, the most well characterised ABC transporters, the expression of which in BBB models is key in evaluating drug transport mechanisms, are P-gp/ABCB1, multi-drug resistance protein (e.g., MRP-1, MRP-5) and breast cancer resistance protein (ABCG2). The function of these transporters can be quantitatively assessed by determining the efflux ratio, which measures the permeability of substances across the transwell semipermeable membrane from apical to basolateral as well as from basolateral to apical compartments [6]. Selective inhibitors can block specific transporters. Therefore, by using these inhibitors, one can categorically identify the transporter to which the given drug molecule binds. P-gp, in particular, can act on a diverse range of drug substrates with very different pharmacophores. The review by Giacomini *et al.* contains details about important efflux transporters that are particularly relevant in clinical pharmacology and drug discovery [32].

Remarkably, contrary to its barrier functions, the BBB has precise mechanisms for supplying nutrients into the brain [33]. For example, small ions and water can pass through by the opening of ion channels and small lipophilic molecules (e.g., ethanol, nicotine, caffeine, barbiturates) are soluble in the hydrophobic lipid membranes of ECs and can enter into the brain by passive diffusion. There are specialised carrier-mediated transporters for transporting polar nutrients, such as glucose (GLUT-1 or SLC2A1), large neutral amino acids (LAT-1) and organic cations and anions (OATP1A2). Some of these transporters also exhibit overlapping substrate specificities. Large proteins (e.g., albumin, histone), hormones (e.g., insulin) and immune traffickers[s1] (e.g., transferrin, IgG) are internalised into the brain parenchyma by receptor- or adsorption-mediated transcytosis. It is to be noted that drugs can be delivered into the brain by utilising one of these transport mechanisms. The *in vitro* model aimed for drug delivery studies must therefore express suitable receptors on the surface of the ECs.

In vitro models of the BBB

Monoculture models

In *in vitro* monoculture transwell models, a uniform layer of BECs is seeded on a semipermeable membrane filter support (Figure 3a) and, depending on the pore size of the filter, cell trafficking experiments as well as drug transport studies can be performed. The BECs cultured can be primary or immortalised cell lines and the model can be constructed using BECs from any animal species (human, mouse, rats, bovine, porcine and monkey) [34]. Monoculture of ECs is the most basic of the BBB models and because of its simplicity it is highly suited for high-throughput screening. However, the major drawback with monolayer cultures is the absence of the influence of other cellular components of the NVU and inadequate barrier properties. Therefore, the most popular *in vitro* models of the BBB are co-culture models that consider the interactions between ECs and the surrounding brain microenvironment.

Co-culture models

In 1987, Janzer and Raff demonstrated that astrocytes could induce BBB-like TJ characteristics in chick ECs of peripheral origin, and in the same year Tao-Cheng *et al.* reported that astrocytes re-enhanced TJ of brain endothelium [35,36]. Ever since the findings from these two independent studies were published, astrocytes or astrocyte-conditioned medium have been extensively used in co-culture models with ECs. A detailed list of endothelial–glial co-culture models including TEERs and effect of permeability on tracer substances are presented in reviews by Deli *et al.* and, more recently, by Wolff *et al.* [37,38]. In most of these models, especially those using primary rat astrocytes, the paracellular barrier properties were significantly improved. The nature of glial cells in endothelial–glial co-culture models can be primary cells of the rat, mice and human/human-fetal or cell lines such as rat C6 glioma, rat CTX-TNA2 and rat SV40. Moderately high TEER (~400–500 $\Omega \cdot cm^2$) and a decrease in permeability of sucrose were observed in bovine ECs co-cultured with rat astrocytes [39,40]. A major advantage of using bovine or porcine ECs over rodents is that a large volume fraction of the brain capillaries can be isolated because of the large size of the brain. Smith *et al.* reported a TEER of 900 $\Omega \cdot cm^2$ on a co-culture model of porcine ECs with rat C6 astroglioma [41]. Recently, maximum TEER in the range 1700–2200 $\Omega \cdot cm^2$ along with extremely low permeability of LY ($P_e = 0.46 \times 10^{-7}$ $cm \cdot s^{-1}$) was documented by Cantrill *et al.* using co-cultures of porcine BCECs with a new immortalised astrocytic cell line CTX-TNA2 from rat [42]. However, it is to be noted that this high TEER of ~2000 $\Omega \cdot cm^2$ was obtained when porcine BCECs were pre-treated with puromycin; the cells untreated with puromycin showed a dramatic decrease in average TEER (182 $\Omega \cdot cm^2$) under similar co-culture conditions. Puromycin has been employed in BBB studies to purify primary BECs, which are often contaminated with astrocytes, pericytes or smooth muscle cells. The idea behind

this operational step is that, because BECs express higher concentrations of P-gp than contaminating astrocytes and pericytes, ECs would resist puromycin treatment by effluxing puromycin out of the cells, whereas the contaminating cells would respond to this treatment and therefore can be easily separated. Moreover, because of the higher P-gp expression, high toxic concentrations of puromycin can be tolerated by the cells. Previous literature evidence has demonstrated a significant rise in TEER for monolayer culture of primary rat BECs purified with puromycin. Also in co-culture models with astrocytes, in the presence of cAMP, puromycin-treated rat brain endothelial monolayer demonstrated reduced permeability to NaF (0.75×10^{-6} cm·s^{-1}) and an increased TEER of 500 Ω·cm^2 [43]. In the aforementioned case, the authors argued that using contaminated primary ECs could affect the barrier integrity of cell monolayers resulting in low TEER (182 Ω·cm^2) [42] and their argument aligns well with previous literature evidence. In addition to puromycin, the astrocytic cell line CTX-TNA2 was also a contributing factor towards tight barrier formation because puromycin pre-treated BEC monoculture showed similar TEER to that of untreated cells in co-culture. Immunocytochemical analysis revealed the expression and localisation of ZO-1 and occludin at the cellular periphery. In co-culture systems, glial cells and also pericytes can be cultured either at the bottom of the well (noncontact configuration, Figure 3bi,biii) or can be seeded at the opposite side of the filter insert in which case they are supposed to interact closely with ECs (contact mode, Figure 3bii,biv). In a comparative study using an *in vitro* co-culture model of primary porcine BCECs with rat glial cells, Malina *et al.* demonstrated that contact orientation produced significantly higher TEER (~1112 ±43 Ω·cm^2) and low paracellular permeability of sucrose (~0.19×10^{-6} cm·s^{-1}) [44]. The model used 10 µm polycarbonate filters with 0.4 µm pore-size. Previous literature evidence demonstrated that pore diameter of 0.4 µm would enable astrocytic foot-processes to pass through the pores and establish physical contact with the ECs seeded on the filter support, whereas the passage of astrocytic cell body to the side of the seeded EC monolayer would be restricted [45]. Moreover, the thickness of 10 µm was just the right distance for astrocyte-released soluble factors, which are relatively short-lived, to reach the seeded endothelial monolayer because they might become inactive while traversing a longer distance of 100 µm from the bottom of the well in a noncontact co-culture system. By contrast, Shayan *et al.* demonstrated, with clear confocal images on a murine back-to-back (contact) co-culture model with rat astrocytes, that on a 0.4 µm diameter filter astrocyte foot-processes actually blocked the pores by passing halfway through them [46]. This not only prevented physical contact of foot processes with the endothelial monolayers but also might prevent the astrocyte-derived soluble factors from reaching the seeded ECs on the opposite side of the filter. Consequently, the authors found no significant difference with regard to barrier tightness and paracellular permeability between endothelial monolayer cultures and contact co-culture configuration. When they tested permeability for a combination of hydrophobic and hydrophilic drugs by culturing astrocytes in a non-back-to-back fashion, the TEER obtained was not significantly high but was comparable to values reported in mouse endothelial co-culture models and, importantly, the model produced an excellent agreement with *in vivo* drug permeability data (correlation coefficient = 0.98) [46]. Concerning the significance of these studies, a key point worth discussing is that astrocytes and ECs are separated by the BM and they are not in contact *in vivo*. Therefore, culturing glial cells at the bottom of the filter to establish physical contact with ECs might not necessarily have a profound impact in influencing EC integrity. Moreover, TEER and permeability values should also be reported with astrocytes cultured at the bottom face of the filter without ECs seeded at the top because the presence of two layers of cells at the bottom and the top could alter model characteristics. Astrocytes can even metabolise certain compounds (e.g., propranolol) and this can introduce artefacts in permeability measurements. However, the clogging of the filters by astrocytic end-feet can serve as a physical barrier towards diffusion of soluble factors into the side of

the cultured endothelial monolayer and thus the contribution of these factors in influencing BBB properties would not be perceived.

In most of these co-culture models, astrocytes seem to modulate the TJ protein expression at the interendothelial cleft thus influencing paracellular permeability; additionally, the efflux transporter expression (ABCB1 and ABCG2) has also been found to be upregulated by astrocytes. Astrocytes also secrete a variety of soluble factors such as glial-derived neurotrophic factor (GDNF), basic fibroblast growth factor (bFGF), interleukin-6 (IL-6), transforming growth factor-β (TGF-β), angiopoietin-1 (Ang-1) and Sonic hedgehog (Shh) [1,47,48]. These factors are strongly believed to influence the maturation and maintenance of the BBB phenotype at a steady-state level [49,50]. Consequently, brain EC monolayers have been cultured in the presence of astrocyte-conditioned media to induce the BBB phenotype *in vitro* [51]. Although these models were unable to display significantly high TEERs, they are usually simple to maintain, culture and mostly compatible with high-throughput screens.

Even though astrocytes have garnered tremendous attention in *in vitro* BBB modelling, studies related to the functional influence of pericytes in the development of fundamental BBB characteristics are rare, with more reports emerging in recent years despite the fact that pericytes are the closest neighbour of the BMECs and they might be the first cell type of the NVU that the developing BMECs come in contact with during embryogenesis when astrocytes are not even differentiated [52,53]. One plausible reason for this lack of study is the absence of brain-specific pericyte markers. However, recent literature suggested platelet-derived growth factor receptor-β (PDGFR-β) could act as a specific marker for unambiguously identifying brain pericytes because mice devoid of PDGFR-β or its binding ligand completely lack brain pericytes [54]. In general, in cell culture models, PDGFR-β is used along with multiple pericyte markers alpha-smooth muscle actin, neuron-glial 2 (NG2) and vimentin for identifying pericytes [55]. Pericytes produce TGF-β, which induced barrier tightness and upregulated P-gp activity in a mouse brain endothelial cell line (MBEC4) co-cultured with rat pericytes [56]. In bovine BCECs, pericytes increased mRNA expression levels corresponding to MRP-6 efflux protein [57]. Nakagawa *et al.* have explored in detail the effect of pericytes and astrocytes by developing tri-culture syngenic *in vitro* models with rat BCECs, astrocytes and pericytes. Out of seven different combinations, involving monoculture, co-culture and tri-culture arrangements, the model that closely resembled the *in vivo* anatomical organisation with pericytes cultured opposite to the seeded endothelial monolayer (contact arrangement, Figure 3ci) and astrocytes at the bottom of the well (noncontact orientation) produced the highest TEER (400 $\Omega \cdot cm^2$) and low paracellular permeability of fluorescein marker ($P_e = 3 \times 10^{-6}$ $cm \cdot s^{-1}$) [58]. In a later study, they characterised this model thoroughly by highlighting the expressions of junction proteins, GLUT-1, efflux transporter P-gp and MRP-1, in addition to obtaining a good *in vivo* correlation with regard to drug permeability studies [59]. In the *in vivo* situation, pericytes establish physical interaction with ECs through peg and socket contacts whereas the space between peg and socket junction contains growth factors (GFs) or signalling molecules that mediate crosstalk between the two cell types [60]. To investigate the effect of EC–pericyte physical interactions on BBB physiology, Vandenhaute *et al.* devised a tri-culture model containing bovine pericytes and BCECs cultured together on the semipermeable membrane for facilitating close interaction, whereas rat astrocytes were cultured in the well (Figure 3ciii). Captured electron microscopic images revealed very close contact between the endothelial monolayer and pericytes and the ECs exhibited low paracellular permeability and expressed efflux transport protein P-gp. However, when this model was compared with the noncontact co-culture setup in which the ECs were seeded on the filter with pericytes and astrocytes at the bottom of the well (Figure 3civ), the paracellular permeability was lower than the close contact model [55].

Most of these tri-culture models utilised bovine or porcine brain BCECs co-cultured with rat astrocytes and pericytes in a calf-serum medium. Therefore, one might not get accurate information when the results from these models are extrapolated to predict the behaviour of drug transport in humans. This prompted researchers to generate all-human mono-, co- and tri-culture models using an immortalised human (hCMEC/D3) cell line, human astrocytic cell lines (CC-2565 and SC-1810) and human brain pericytes [61]. This model [s2]closely resembled Nakagawa's tri-cultivation model applied on an all-human set-up [58]. The cells were allowed to grow in the cell culture medium containing human serum. Surprisingly, the tri-culture model involving all three cell lines with pericytes seeded at the bottom of the filter, allowing close contact with ECs, proved to be inferior to the co-culture models using either astrocytes or pericytes. Moreover, the astrocyte contact co-culture conditions produced higher TEER than pericyte co-culture even though the highest TEER value measured was less than 100 $\Omega \cdot cm^2$ [54]. Therefore, it can be concluded from their findings that the barrier tightness in a human *in vitro* BBB model is effectively lower than that of other species, and the inclusion of pericytes does not enhance the formation of TJs in contrary to what Nakagawa and co-workers have observed in their models. However, throughout this study, apart from TEER, no other measurements such as permeability of tracers or analysis of the expression of TJ proteins and transporters were conducted. Thus, no other significant parameters can be taken into guidance to support any major conclusion derived from this study.

Neurons maintain close association with astrocytes and hence can indirectly regulate BBB permeability by modulating the properties of ECs through astrocytes. Hence, it is more sensible to setup tri-culture models of neurons with astrocytes to analyse the synergistic influence of neurons and/or [s3]glia on EC permeability. A syngenic tri-cultivation model developed from rat primary BMECs, astrocytes and neurons recorded an increase in TEER by 35.9% (actual value = 268 $\Omega \cdot cm^2$) when compared with endothelial monoculture and co-culture models involving either astrocytes or neurons with BMECs. Notably, the model also demonstrated increased expression of P-gp transporter and ZO-1, as well as low permeability to NaF [62].

A significant number of the co-culture models described above have produced suboptimal TEER values, which is substantially lower than what is found *in vivo*, high paracellular permeability, lack of expression of important transporters, enzymes and inconclusive data arising from lack of reproducibility under similar experimental paradigms. It is also noteworthy that, even though many details of the astrocytic influence in modulating EC behaviour are unknown, as a general trend astrocytes have performed consistently better in improving TEERs than pericytes. It is well accepted that glial cells can induce the expression of TJ proteins, efflux transporters and enzymes in BECs and thereby aid in barrier tightness [1]. However, it is too early to undermine the role of pericytes because elaborate studies need to be conducted to unravel the exact contribution of astrocytes and pericytes in forming a restrictive barrier. In this regard, it can be argued that the mechanism of pericyte differentiation must be taken into account when establishing models containing pericytes. For example, information gathered from the literature suggested that pericytes differentiated with TGF-β could negatively affect TEER, whereas pericytes differentiated with bFGF were found to increase TEER [63].

Human cell-based models

Immortalised cell lines. Human cell-based BBB models are important for translation of therapies to humans, because there are differences among transporter genotypes between human and other species. To investigate delivery of drugs to the human brain, it would be ideal to use primary human BECs (hBECs) because it would eliminate interspecies variations; but, as a result of stringent regulations and restrictions, it is difficult to experiment with hBECs. Moreover, the source of obtaining human primary cells is from cryopreserved tissues that had been removed surgically and

hence they might not be regarded as healthy cells. Because access to healthy human BBB tissue is restricted on ethical grounds, to date only a few immortalised cell lines have been developed to generate human BBB models *in vitro*. The HCMEC/D3 cell line was first reported by Weksler *et al.* in 2005, and since then more than 100 publications have reported using this cell line for understanding the mechanisms associated with CNS pathology, immune response and drug transport studies [64,65]. As a result, the HCMEC/D3 cell line is extensively characterised compared with all other human immortalised cell lines. This cell line expresses important endothelial markers including CD34, CD31, CD40, CD105, CD144 and the von Willebrand factor; by comparison, another human cell line (HBEC-5i) does not show positive staining for the CD31 marker [65,66]. Moreover, hCMEC/D3 monolayers express important TJ proteins and are reported to form a tight and effective barrier for compounds with high molecular weight, as demonstrated by lower permeability values for 4 kDa dextran (5–13 × 10^{-6} cm·s^{-1}) and 70 kDa dextran (0.2–0.3 × 10^{-6} cm·s^{-1}). In fact, for compounds having MW ≥4000 kDa, paracellular permeability closely resembles the profiles reported for well-characterised bovine and porcine models. Additionally, expression of 44 SLC transporters (GLUT-1, LAT-1 and MCT family transporters), receptors such as insulin and transferrin and 23 efflux transporters of the ABC family, which include P-gp, MRP-4 and BCRP, has endowed this cell line particularly amenable for drug uptake and active transport experiments [26,67]. However, a major area of concern that can limit its potential for routine use is the low TEER range (30–50 Ω·cm^2) and enhanced permeability of paracellular markers with low molecular weight – sucrose, mannitol, NaF and LY – average range (20–90 × 10^{-6} cm·s^{-1}). In this regard, it has been observed that treatment with the anti-inflammatory steroid hydrocortisone, or addition of lithium chloride (LiCl) which can induce Wnt/β catenin canonical signalling, can increase TEER [68]. This signifies that modulation of TJ protein expression associated with barrier tightening is necessary to improve TEER. This observation is also supported by a study in which detailed transcriptional profiling at the mRNA expression level was performed on HCMEC/D3 cells and then this profiling was compared with published data available for freshly prepared mouse BECs [69]. The TJ proteins, specifically Claudin-5, occludin, as well as some members of SLC and ABC family transporters, were found to be expressed in low levels compared with mouse BECs. Probably, addition of hydrocortisone or Wnt activator LiCl increased the expression level of Claudin-5 or occludin, thereby enhancing TEER. Pollar *et al.* have reported a decrease in sucrose permeability 39 times by substituting fetal bovine serum (FBS) with human serum in the cell culture medium [70]. The all-human tri-cultivation model used human serum, but sucrose permeability was not determined to evaluate its effect. Another human cell line BB19 was developed as early as in 1996, but its use is limited because of high sucrose permeability [71,72]. No permeability data were reported for human cell lines NIKM-6, HCEC, HBEC-5i and HBMEC-3 [65,66,73,74]. The HBMEC-3 cells also lack any phenotypic characterisation. The TY08 cell line showed lower levels of P-gp expression and permeability coefficient 1.23 × 10^{-3} cm·s^{-1} for inulin tracer [75,76]. The recently developed HBMEC/ciβ cell line showed initial promising data, in terms of endothelial expression markers, proliferation capacity and expression of TJ proteins, P-gp and BCRP; but an average value for TEER was not reported, although it was mentioned that the TEER was poor, indicating low barrier strength. The paracellular permeability of sucrose was also several-fold higher than that *in vivo* [76]. The TY10 cell line immortalised by transduction of temperature-sensitive SV40 large-T antigen showed initial promise in their ability to express Claudin-5, occludin and ZO-1. At 33°C these cells were able to retain their morphology up to 50 passages, but when the temperature was shifted to 37°C loss of SV40 large-T antigen occurred [77]. To optimise a cell line for high- to medium-throughput permeability screening, a comparative study using four different human immortalised cell lines (hCMEC/D3, hBMEC, TY10 and BB19) was performed on a 24 well plate format. The best optimised model in terms of highest TEER (40 Ω·cm^2) and lowest paracellular permeability of LY (5.39 ±0.364 × 10^{-6} cm·s^{-1}) was obtained with hCMEC cell lines in monolayer

cultures on a transparent PET membrane of 3 µm pore size. However, hCMEC/D3 and hBMEC cell lines expressed AJ proteins, as well as ZO-1, whereas TY10 along with hCMEC/D3 were able to express Claudin-5, which was also detected in low amounts in hBMEC [78]. The TEER for monolayer culture was measured using cellZscope®, hence it cannot be compared with TEERs reported previously for monolayer culture of these cell lines using EVOM. The measurements in this study were done using several culture inserts, bought from different suppliers and of varying filter sizes, different cell seeding density and in the presence of several growth media to optimise the best possible conditions in terms of achieving highest TEER and lowest parcellular diffusion. Surprisingly, no change in TEER was observed upon replacing FBS with human serum. This could be caused by variation in the FBS composition attributed to different commercial sources. Interestingly, tri-cultivation of these cell lines in the presence of astrocytes (SVG-A cell line) and human pericytes (HBPCT cell line) showed no improvement in TEER, an observation that is consistent with previous study results [39,40]. It is to be noted here that TEER for the triple culture model was measured with EVOM because the cellZscope®, owing to its basic design, does not support the format in which cells are seeded at the bottom [78].

Stem cells. Human immortalised cell lines can act as substitutes for primary cells but, as discussed above, they do suffer from serious limitations, the primary drawback being their inability to form a tight barrier under optimum culture conditions as indicated by inferior TEERs relative to an *in vivo* environment [65,78]. Under such a scenario, human stem cells are the best resources for generating human brain-like endothelial cells (hBLECs) in large scales. In stem cell culture models pioneered by Shusta and co-workers, hBLECs were obtained by the differentiation of human pluripotent stem cells (hPSCs) [8,79]. Under contact co-culture conditions with neural cells, the BLECs acquired strong paracellular barrier functions (TEER = 1450 ±140 $\Omega \cdot cm^2$) with expression of well-defined nutrient and efflux transport systems [8]. In a further complex mixed culture adaptation of this model, the hBLECs were derived from retinoic-acid-treated hPSCs and were allowed to grow in the presence of neural progenitor cells that differentiated into astrocytes, pericytes and neurons. Retinoic acid was used to improve the BBB phenotype of the ECs by increasing occludin and VE-cadherin expression. The peak TEER recorded for this model after 25 h of culture was extremely high (5000 $\Omega \cdot cm^2$) [79]. To date, [s4]this is the highest TEER recorded by an *in vitro* BBB model. Even though these innovative stem cell culture BBB models displayed impressive barrier characteristics, and can meet the demands for large-scale production of *in vitro* BBB models, the models suffer from some serious drawbacks: the differentiation process involving the stem cells was complex and the peak TEER started to decrease after 50 h of culture. The TEER was also dependant on the initial source of hPSCs. Moreover, the phenotypic characteristics of the cellular components were not adequately described and the *in vitro* permeability data were compared with rat *in vivo* uptake and not human. The other two stem cell models used human cord hematopoietic stem cells to derive hBLECs. One study demonstrated upregulation of occludin, GLUT-1 and P-gp in hBLECs derived from human endothelial progenitor cells and co-cultured with astrocytes for 15 days. However, the TEER measured for this model was very low (60 $\Omega \cdot cm^2$) and the optimum paracellular permeability was sustained for only 4 days. Additionally, *in vivo* correlation comparison profile related to the permeability measurement was not described [80]. The other study is comparatively more relevant, because it is the first study of its kind to obtain a correlation coefficient (0.89) with *in vivo* human permeability data [7]. The TEER reported for this model was 175 $\Omega \cdot cm^2$ and the authors demonstrated that the induction of barrier properties was at least in part mediated by the clues provided by the canonical Wnt signalling pathway from pericytes. This is a significant finding related to understanding the underlying mechanisms of regulating BBB phenotype and functions by pericytes. Prior studies have associated angiopoietin-1 and TGF-β secreted from pericytes in inducing TJ and regulating normal functions of

the BBB [56,81]. But this is the first time the Wnt signalling pathway has been associated with pericytes in developing BBB properties *in vitro*. Also, this model is highly reproducible because it was reproduced in several laboratories using stem cells from different donors. The model could retain the optimal paracellular permeability value of LY for 20 days and thus can be considered stable for at least 20 days. In principle, this model presents many attributes of a promising human *in vitro* BBB model for standard use in drug discovery programs – stability, scalability, reproducibility and a good correlation with human *in vivo* permeability. However, the TEER for this model is still relatively low in comparison with the *in vivo* situation, and the permeability coefficient has been reported for only nine compounds, which by no means is exhaustive enough to conclude the true predictive potential of this model for testing permeability of a new generation of CNS therapeutics.

Dynamic models

The BECs use a hollow cylindrical geometry and operate in a laminar flow regime. The BECs respond to the effect of shear stress by redistribution and flattening of cell fibres (structural remodelling) or in other words shear stress can regulate the functions and morphology of the BBB [82]. The 3D dynamic BBB models have definitive advantages over 2D models because they allow researchers to study the effects of confinement, geometry and flow conditions on cell behaviour. Confinement is important to recreate the constriction of the flowing blood cells in the capillaries by the vessel walls. It is impossible to reproduce the effect of confinement in 2D models. The *in vivo* blood flow confined to a hollow cylindrical capillary was mimicked *in vitro* by culturing BECs on the inner surface of cylindrical hollow fibres. The outer surface of the hollow fibres was coated with poly-D-lysine (PDL) which supports co-culture with astrocytes. A bundle of these hollow fibres was placed inside a sealed chamber supplied with electrodes for continuous TEER monitoring (Figure 4). The cell culture medium circulating inside the hollow tubes could generate a physiologically relevant shear stress of ~5 dyne·cm^{-2}. The use of these 3D artificial hollow fibres representing capillary-like geometry provided larger surface area for cell–cell communication and improved shear environment. This kind of model was initially developed and studied extensively by Cucullo *et al.* [83]. By applying flow conditions on primary human BECs co-cultured with astrocytes, a TEER of 1000 Ω·cm^2 was recorded; sucrose permeability was below 2×10^{-7} cm·s^{-1} [84]. Under similar conditions, human immortalised hCMEC/D3 cell lines also recorded a similar TEER, a substantial improvement compared with static models, but the astrocytes co-cultured with hCMEC/D3 seemed to have no effect in influencing TEER [85]. Despite obtaining high TEERs with human cells, the dynamic model has many specific disadvantages as outlined by Naik and Cucullo: substantial amounts of cells are required to fill the large capillary volumes, real-time monitoring of cell behaviour in the inner luminal surface is impossible, high-handed technical skills are needed to set up the model and, compared with conventional static transwell systems, this apparatus is incompatible with high-throughput pharmaceutical screening [11].

The microfluidic device uses small fluid volumes and therefore requires fewer cells. Also, the ECs can be exposed to a physiologically relevant sheer stress benefitting from a well-defined laminar flow offered by the microfluidics. This model system was found to increase TEERs for human hCMEC/D3 cell lines (from 40 Ω·cm^2 without sheer to 120 Ω·cm^2) and seemed to upregulate ZO-1 expression in the endothelial membranes [9]. Another benefit of microfluidic models is that visualisation of cells is made possible by the transparent nature of the materials used. However, in spite of promising benefits and outcome, the model is unable to reproduce the exact geometry of the *in vivo* microvascular phenotype and the TEERs reported were not extraordinary (250–300 Ω·cm^2) compared with other forms of existing *in vitro* BBB models [9,86,87].

Assessing nanocarrier permeability using *in vitro* BBB models

Because lipophilic drugs can cross the BBB more easily through passive diffusion, one strategy would be to modify hydrophilic drugs by attaching chemical moieties that would make the overall molecule nonpolar. The downside of this modification is nonselective delivery and unwanted accumulation of drug in peripheral organs. Other strategies that can be undertaken include inducing temporary or transient disruptions of the BBB resulting in increased permeability. The stimuli for this type of disruption could include chemical agents that can reversibly modulate TJ and AJ proteins and increase temporarily paracellular permeability aiding in the diffusion of the drug [88].

Stimuli of the physical origin such as application of ultrasound can also cause temporary reversible disruptions of the junction proteins [89]. However, this temporary noninvasive disruption carries a significant risk and the extent of the disruption needs to be strictly controlled. The most useful strategy in this regard is a targeted delivery approach in which the drug is formulated in a suitable vector that can cross the BBB by receptor- or absorption-mediated transcytosis [90,91]. Examples of such nanocarriers include liposomes, micelles, polymeric nanoparticles, dendrimers, quantum dots, iron oxide or metal-based nanoparticles and nanoparticles composed of solid lipids [92]. Although simple cost-effective models are desirable for medium- to high-throughput screening, more complex co-culture models have been more popular for evaluating nanoparticle delivery. Some examples of nanoformulations, and the commonly employed *in vitro* BBB models used for testing their penetration ability, are illustrated in Table 1. Among different cell types, the popular choice is primary BECs from rat, mouse, bovine, porcine and human, whereas human and rat immortalised cell lines HCMEC/D3 and b.End3, respectively, have been used in testing many of these nanoformulations with or without cargoes loaded. Surprisingly, immortalised cell lines from noncerebral origin such as Madin–Darby canine kidney (MDCK) and human colorectal adenocarcinoma (Caco-2) have also been used for testing drug permeability because these cell lines form tight monolayers under suitable culture conditions [93,94]. However, the fundamental disadvantage of using these cells of epithelial origin is the display of completely different phenotypic morphology in culture – narrow tall [s5]verses usual long spindle shapes for BECs. The primary expectation from using *in vitro* models is to identify an optimal formulation that subsequently would demonstrate equivalent *in vivo* efficacy. In an excellent review by McCarthy and colleagues, a comparison with *in vivo* data for some of these formulations tested using *in vitro* models is provided, and the results show that in some specific cases *in vitro* experiments were successful in identifying formulations that would demonstrate enhanced *in vivo* efficacy [95]. This seems encouraging, but translation of these results from animal models to humans still remains a major hurdle to overcome and the root of this challenge lies in the development of human *in vitro* models adequately reproducing important human BBB phenotype and functions. Although some of these therapeutics encapsulated in liposomes have made it to Phase I and Phase II clinical trials (https://clinicaltrials.gov), as of yet no therapeutics in nanoformulations are available on the market to treat CNS-related disorders [95].

BBB basement membrane

The BM is the noncellular counterpart of the NVU and at the BBB level there are two distinct BMs in close contact with each other and apparently they cannot be differentiated under a light microscope. The endothelial BM separates ECs and pericytes, whereas the parenchymal BM (also known as glia limitans/astrocyte BM) separates astrocytes from ECs. The two BMs have different compositions based on laminin isoforms. Laminins are glycoproteins containing three subunits (α, β and γ; Figure 5b) and, depending on the combination of these subunits in different stoichiometric ratios, formation of several isoforms is possible. The laminin isoforms 411 (α4β1γ1) and 511 (α5β1γ1) are secreted by the ECs and they form the major constituents of endothelial BM, whereas parenchyma BM is primarily composed of laminin 111 (α1β1γ1) and 211 (α2β1γ1) isoforms, which are secreted

by astrocytes [96,97]. Besides laminin, other key components of the BMs are network forming collagen type IV (Figure 5a), fibronectin, nidogen and heparan sulfate proteoglycans (e.g., agrin and perlecan). All these components of the BM undergo spontaneous self-assembly into higher order networks. Nidogen and perlecan spontaneously bind to each other, and then form a bridge between laminin and collagen IV, where nidogen is connected to the Y chain of laminin (Figure 5c). Importantly, cells actively support the self-assembly of BM components through mediation of signals to and from the cell cytoskeleton with the help of cell-surface receptors [98,99]. This complex self-assembly process is pictorially represented through simplified sketches shown in Figure 5d.

Many of these extracellular matrix (ECM) components are natural ligands for receptors expressed by the abluminal membranes of the capillary ECs, as well as astrocytes and pericytes. These receptors are mostly different subclasses of integrins such as α1β1, α6β1, α6β4, α3β1, αvβ1, αvβ3, α5β1 and α4β1 and dystroglycans [100]. Besides matrix receptors, the ECs also express important GF receptors on their surface for binding soluble factors released from pericytes and astrocytes. The BMs are endowed with the ability to entrap these soluble factors released from cellular components of the NVU. These can include TGF-β and Shh, secreted by pericytes and astrocytes, Ang-1 released from pericytes and Wnt secreted by astrocytes. The binding of these GFs, as well as ECM components, to their corresponding receptors expressed by ECs can induce important cell signalling events leading to upregulation of important TJ proteins resulting in barrier tightness [101]. For example, agrin receptors are expressed by ECs and the binding of agrin to its receptor can upregulate the expression of TJ proteins Claudin-5 and occludin. In glioblastoma, when agrin is lacking, Claudin-5 and occludin expressions are also supressed [102]. Depletion of agrin could also cause depolarisation of astrocytic end-feet primarily by perturbing the distribution of aquaporin 4 (AQP4) [103]. Perlecan is another major functional unit of the BM because it interacts and grounds several GFs including vascular endothelial growth factor (VEGF), PDGF and TGF-β in the ECM [104]. During stroke, perlecan undergoes proteolytic cleavage and some of these cleaved products, particularly the protein fraction containing C-terminal domain V (DV), can be beneficial for restoring motor function and reducing glial scars [105]. Laminins also play an important part in promoting BBB tightness. Laminins bind to integrin subtypes containing β1 chains and this binding mediates EC attachment to the BM promoting Claudin-5 localisation at the TJ. When β1 integrins are blocked, the expression of Claudin-5 gets suppressed resulting in the increased paracellular permeability of the endothelial barrier [106]. Interestingly, a recent report has claimed that laminin-111 of the glia limitans maintains BBB integrity by preventing the differentiation of pericytes from the resting stage (stable) to the contractile or BBB-disrupting stage [107]. It has been demonstrated that pericytes release Ang-1, which can upregulate the gene encoding TJ protein occludin by activating the Tie-2-mediated signalling pathway [81]. In recent years, Wnt/β-catenin-mediated signalling has been recognised as the major player in inducing BBB characteristics in the developing brain, as well as maintaining the barrier phenotype in adulthood [108]. The astrocytes release Wnt ligands, which are then trapped by the BM matrix as they undergo post-translational modification [109]. The inhibitory factors of Wnt render them inactive whereas TGF-β signalling triggers their activation by reducing the concentration of Wnt inhibitors thus releasing Wnts from the matrix [110]. The Wnt ligands bind to their target receptors (Frizzled 4 and LRP/6) expressed by the ECs and the binding interaction initiates the β catenin signalling pathway, resulting in the transcription of genes encoding TJ proteins [17]. Moreover, injection of soluble inhibitors of Wnt *in vivo* has been found to generate vascular defects and breakdown of the BBB [111]. This evidence strongly suggests that Wnts are involved in the regulation and maintenance of normal BBB functions. Another important morphogen secreted by astrocytes and pericytes on the BM matrix is Shh, which can bind to Patched-1/[s6]Smoothened[s7] receptors on the endothelial membranes and can modulate the expression of TJ proteins by activating specific transcription factors such as Gli-1 [112]. The complex bidirectional crosstalk

between the BMs and cellular components of the NVU using soluble factors as the mediators is depicted in Figure 6.

Cell-support materials can regulate NVU functions

Because the binding of the natural constituents of the BMs to the matrix receptors on the surface of the endothelial membranes promotes cell adhesion, growth, proliferation and migration, the BM components, in particular collagen, laminin and fibronectin, are often used as scaffold materials to mimic the function of these proteins in *in vitro* BBB cultures. Tilling *et al.* first systematically investigated the influence of cell-support materials in regulating TEER *in vitro* using porcine brain endothelial cell monolayers. Cells seeded on type IV collagen, fibronectin, laminin and a combination of all three proteins in the ratio of 1:1:1 showed elevated TEERs in comparison with cells cultured on rat tail collagen type I [113]. Interestingly, type I collagen is not naturally present in the brain BM. In another study, RBE4.B cell lines grown on collagen type I coated matrix failed to show mRNA expression coding for occludin, whereas collagen type IV or laminin coated substratum were able to trigger occludin mRNA expression [114]. These results indicate that cell culture scaffold materials can influence the tight barrier formation. By contrast, in the study reported by Vandenhaute *et al.* three different coatings (Matrigel®, laminin and PDL) were used in the following combinations: (i) Matrigel® on top face; (ii) laminin + Matrigel® on top face of filter membrane; (iii) PDL on bottom face of filter and Matrigel® on top; and (iv) PDL at bottom, layer of laminin and Matrigel® on top face. Surprisingly, this study failed to demonstrate any significant effect on membrane permeability of LY, but showed EC monolayer invasion and growth of a second monolayer at the filter bottom face filter and the expression of ZO-1 [28]. Irrespective of the nature of coating used, the double layer of endothelial growth was prevented by culturing solely ECs with a dry bottom for one week followed by seeding of pericytes to achieve co-culture conditions. From this study, the authors concluded that the mechanism of EC invasion was physical and not biochemically controlled by coating of the insert. Thus, the nature of the cell culture coating might not influence the migratory aptitude of ECs *in vitro.* However, to date, the precise mechanism of interaction between BBB BM and the NVU components is still not clear and more-elaborate studies in this avenue remain to be done. In a study by Hartman *et al.*, porcine BCECs were allowed to grow on an ECM deposited by astrocytes and pericytes. The TEER was then compared with cells grown on matrices produced from brain and non-brain ECs and it was significantly higher for ECs cultured on the glial-derived ECM. This proves that the components of the astroglial BMs are particularly essential for controlling BBB tightness [115]. Recently, an elegant study has shown that BM proteins can regulate the astrocytic phenotypic morphology in *in vitro* cultures. When human fetal-derived astrocytes were cultured on different cell culture coating materials – Matrigel®, fibronectin, collagen IV and collagen I – the best astrocyte-like morphology involving protrusions and branchings was displayed on Matrigel®-coated surfaces [116]. In a recent follow-up study, this group fabricated a newly designed matrix comprising hyaluronic acid polysaccharide, Matrigel® and collagen. The human fetal-derived astrocytes grown on this matrix not only developed star-shaped morphology with radial processes but also maintained normal expression levels of glial fibrillary acidic protein (GFAP) [117]. Surprisingly, before this study, the astrocyte phenotype was hardly described in most co-culture BBB models with brain ECs. In fact, rat astrocytes frequently co-cultured with BMECs were reported to adopt a rounded morphology with short processes and also showed elevated levels of GFAP [118]. These are interesting results unambiguously pointing towards the fact that the composition of the cell culture matrix can guide the differentiation of cells into their true phenotype in *in vitro* cell culture models.

New outlook for *in vitro* BBB modelling

Even though during the past decade a tremendous amount of research effort and resource has been invested in developing new cell culture models of the BBB with strong barrier characteristics that persist *in vivo*, a model that can be recognised as the gold standard for predictable high-throughput screening application has not yet been reported. A major area of concern that remains consistent in the majority of these BBB *in vitro* cell culture models is the lack of reproducibility in experimental outcomes. Related to this concern, a significant area of development that has been mostly overlooked is the introduction of novel cell culture platforms for generating BBB models. The standard coating materials that have been applied on filter supports for seeding BECs reported to date are rat tail collagen type I, collagen type IV, fibronectin, gelatin, mouse laminin, Matrigel® and PDL. An exhaustive list of cell culture materials used for establishing *in vitro* BBB models is summarised and presented in a tabular form by Bicker *et al.* [51]. Interestingly, PDL is not a natural component of the BM and gelatin is denatured collagen. If we recollect the information presented by Hartman *et al.* [115], then these materials might not be considered as desirable for imparting strong barrier characteristics. Also, collagen type I has been most widely used as a cell support material in BBB models. Although collagen type I can provide structural support to the cells, it has fibrillar architecture contrary to natural BM collagen type IV, which forms a higher order polygonal network structure (Figure 5a). Hence, the structural characteristics of cells growing on membranes coated with collagen type I are not even similar with the natural BM of the NVU. An effect of this structural dissimilarity in BBB models is reflected by the findings reported by Tilling *et al.* as described earlier [113]. Interestingly, astrocytes cultured on Matrigel® support were able to reproduce some of the best phenotypic characteristics and yet Matrigel® represents the BM extracted from mouse tumour, and hence has the potential to introduce diseases. Similarly, collagen type IV is usually obtained from animal species, such as bovine, and chances are it can elicit immunogenic responses. Moreover, because these natural ECM components are isolated from different animal sources they are heterogeneous or do not have a fixed composition and this batch-to-batch variation in their composition could easily affect the overall reproducibility of experimental results. Consequently, the lack of reproducibility in data obtained from *in vitro* cell culture models is still the major hurdle that has prevented their customisation as robust *in vitro* models for routine drug screening. Additionally, large proteins, such as collagen and fibronectin, are difficult to modify because they tend to denature and often lose their mechanical properties when subjected to chemical modification.

An alternative strategy would be to engineer novel cell culture platforms from synthetic building blocks that will mimic the structure and functions of the BBB BMs and still be nontoxic. Natural or synthetic polymers, peptide amphiphiles (PAs) or even polymer peptide conjugates can be considered for this type of design purpose. However, the most challenging part in constructing an artificial BM is to mimic the hierarchical organisation of the membrane architecture, while at the same time the membrane should be bioactive so that the cells can respond to cues provided by the membrane. In principle, we can readily obtain nanofibres by the self-assembly of rationally designed PAs and, depending on the in-built peptide sequence, the nanofibres could even respond to cellular cues; however, in most cases, the self-assembly is more likely to produce hydrogels rather than stable membranes [119,120]. Conversely, a recent paper has documented a synthetic self-assembly approach for the generation of mechanically stable membranes from peptide–polymer mixtures. The authors used electrospinning processing to induce fibre formation and, because the membranes contain bioactive peptide sequences, they supported the adhesion, growth and long-term culture of primary renal epithelial cells displaying strong barrier properties [121]. Recently, our group has reported the design of self-assembled bioactive robust membranes by simple mixing of hyaluronic[s8] acid with β-sheet fibril forming PA incorporating a matrix metalloproteinase (MMP)-1-sensitive sequence. The membranes supported the adhesion and growth of dermal fibroblasts and underwent

slow degradation when treated with recombinant MMP-1 *in vitro* [122]. Therefore, implementing a self-assembly strategy for forming higher-order BM network structures will be a promising approach for generating artificial BMs of the BBB. Integration of small peptide epitopes such as cell adhesion sequence or specific GF-binding sequences (e.g., TGF-β) into these self-assembled membranes can render the scaffold bioactive and attractive for GF binding. Consequently, now the scaffold can mediate cell adhesion and regulate cell signalling events through controlled local release of bound GFs. Because the cellular components of the BBB communicate with each other through release of soluble factors, which are captured and released by the BMs, the incorporation of this feature into an artificial BM construct will induce barrier tightness by regulating the expression of TJ proteins. Moreover, the composition of a synthetic BM is fixed, maximising the reproducibility of experimental outcomes. Thus, an *in vitro* BBB model recreated on an engineered artificial synthetic membrane support can be considered as more predictable than when natural protein components of the ECM matrix are used as scaffold materials for cell growth. Depending on how well the cells communicate with these artificial membranes, the *in vitro* BBB model can be fine-tuned for customisation for routine use in high-throughput studies in drug discovery and development research.

Lastly, the BBB microvasculature is composed of arteries, venules and capillaries and a certain level of heterogeneity is expected for ECs isolated from these sources in terms of physiological properties. For example, ECs extracted from capillaries are comparatively less permeable than ECs from arterioles and venules [123,124]. Considering this viewpoint, we can assume that a level of overall heterogeneity in the composition, morphology and functions of the BM exist depending on their anatomical localisation in the microvasculature. Although this variability can impose a formidable challenge when considering the design of a new BM, on the brighter side, because the BM will be synthetically constructed, one can manipulate the choice of bioactive materials taking into account the composition at different subanatomical sites.

Concluding remarks

In vitro BBB models are indispensable screening tools for determination of drug delivery into the brain. In recent decades, intense research has produced some impressive *in vitro* cell-based model systems, some novel, whereas others improved variations of pre-existing models. Each model system comes with its own ingenious design, applications and limitations (Table 2). However, a common fundamental feature that is ubiquitous in these models is the lack of better cell-support materials that can mimic more accurately the organised structure and functions of the BBB extracellular environment. Thus, we foresee a new area of advancement through construction of artificial bioactive membranes that can emulate the performance of the BBB BM. Moreover, the core value of this approach lies in the fact that already established and potential *in vitro* models can be regenerated on these new cell culture platforms with a promise of gaining higher predictability and a possible pathway leading towards customisation in pharmaceutical research.

Acknowledgements

H.S. Azevedo acknowledges the financial support of the European Union under the Marie Curie Career Integration Grant SuprHApolymers (PCIG14-GA-2013-631871). J. Banerjee is supported by Marie Sklodowska-Curie Individual Fellowship granted by the European Commission (MSCA-IF-2014-658351) and Y. Shi acknowledges China Scholarship Council for her PhD Scholarship. We are highly grateful to Fan Wang, PhD student, and Dr Nicolas Raske, Postdoctoral Research Fellow, from School of Engineering and Material Science, Queen Mary University of London, for helping us in the modification of Figure 2 and proof-reading the manuscript, respectively.

Figure legends

Figure 1. [s9]Schematic[s10] representation of the neurovascular unit (NVU) at the site of the brain capillaries: the cerebral blood capillaries in the brain are lined by a continuous layer of endothelial cells (ECs) surrounded by the endothelial basement membrane (BM), in which the brain pericytes are embedded. The astrocytic end-feet surround the ECs but are not in direct contact with them; instead the BM separates the astrocyte foot processes from the ECs. The astrocytes also maintain close association with the neurons. Microglia are the immune cells of the central nervous system (CNS). Occasionally, there are gaps or discontinuities in the astrocytic end-feet coverage where neurons and microglia can innervate the BM. Note: the capillary lumen and walls, and the BM, are relatively scaled, but other components of the NVU are indicated, but not scaled. Adapted, with permission[s11], from [1,150].

Figure 2. Transwell culture system typically used in *in vitro* blood–brain barrier (BBB) models and measurement of trans-endothelial electrical resistance (TEER) employing traditional chopstick electrodes of the voltohmmeter type (EVOM). Transwell plate with a total of six (ai), 12 (aii) or 24 (aiii) wells containing a porous filter insert (aiv) which divides the transwell into upper apical or blood compartment and lower basolateral or brain compartment. (bi) Measurement of TEER for a porous semipermeable membrane insert (control); (bii) a uniform layer of brain endothelial cells (BECs) are seeded on the top of the filter membrane coated with an extracellular matrix (ECM)-derived protein (e.g., collagen I, collagen IV, laminin, fibronectin, gelatin from rat or bovine), Matrigel® or Matrigel™ [s12][a solubilised basement membrane (BM) preparation extracted from the Engelbreth-Holm-Swarm mouse sarcoma, a tumour rich in ECM proteins such as laminin, collagen IV, heparin sulfate proteoglycans, nidogen and a number of growth factors (GFs)], matrices deposited by cultured astrocytes or pericytes or synthetic poly-D-lysine (PDL). TEER of confluent endothelial monolayer is recorded by placing two electrodes, one on each side of the transwell compartments as shown. (ci) Measurement of TEER with astrocytes seeded at the bottom face of filter (control); (cii) TEER measurement of a typical contact co-culture system. Adapted, with permission, from [3,6].

[s13]Figure 3. Mono-, co- and tri-cultivation models of the blood–brain barrier (BBB). (a) Mono-culture model: the endothelial monolayers are cultured on transwell membrane insert. (bi) Endothelial–glial co-culture model in non-contact configuration. Astrocytes are cultured on the bottom of the transwell, whereas endothelial monolayer is cultured on top of the filter membrane; (bii) endothelial–glial co-culture in contact orientation. The astrocytes are seeded on the bottom of the filter membrane so that they are in close proximity with the endothelial cells (ECs) cultured on top of the filter; (biii) co-culture of pericytes at the bottom of well; (biv) contact co-culture model with pericytes. (ci) Tri-culture model involving ECs, astrocytes and pericytes with pericytes cultured on opposite side of filter; (cii) another format of tri-cultivation model. Here astrocytes are in contact orientation and pericytes cultured at the bottom of the well; (ciii) pericytes and ECs are in very close contact and astrocytes cultured at the bottom. This configuration very closely mimics the *in vivo* anatomical organisation of the neurovascular unit; (civ) non-contact format of tri-culture model involving ECs, astrocytes and pericytes. Adapted, with permission[s14], from [12,55,58].

Figure 4. [s15]Schematic representation of dynamic *in vitro* blood–brain barrier (BBB) model. The endothelial cells (ECs) are cultured inside the fibronectin-coated surface of hollow fibres made up of polypropylene. This system allows co-culture, because astrocytes can be cultured on the outer surface of the hollow fibres. A single hollow fibre is highlighted in yellow. A bundle of these hollow

fibres is then packed inside a sealed chamber. The cell-culture medium is pumped through the chamber by a pump with adjustable speed control. The pulsatile flow of the cell-culture medium mimics the flow environment that persists *in vivo*, and helps to generate the sheer stress. Adapted, with permission, from [s16][11].

Figure 5. [s17]Supramolecular assembly of basement membrane (BM) and its major components: collagen IV, laminin, nidogen, agrin and perlecan. (a) Collagen IV network formation: an assembled protomer contains a triple helical domain flanked by a short 7S domain at the N-terminal and a noncollagenous globular trimeric domain (NC1) at the C-terminal. The NC1 domains of two protomers interact to form NC1 hexamers (dimer). Next, four protomers interact at the 7S domain to form tetramers (ordered lattice structure), adapted, with permission[s18], from [151]. (b) Laminin network formation through polymerisation: cruciform structure of laminin containing α, β and γ chains. Typically, α-chain of laminin contains a domain that binds other extracellular matrix (ECM) proteins, an α-helical region and an integrin-binding domain. Primary interactions lead to a trimer formation, by the binding of three different domains, followed by polymerisation, adapted, with [s19]permission, from [152]. (c) Complex molecular interactions among different components of the BM directing the self-assembly process: nidogen and perlecan mediates laminin-collagen IV binding whereas agrin binds to laminin, adapted, with [s20]permission, from [153,154]. (d) Agrin and the laminin network are anchored to the cell surface by interactions with integrins, α-dystroglycan and sulphated glycolipids/sulfatides. Adapted, wit[s21]h permission, from [154,155]

Figure 6. Involvement of the basement membrane (BM) in complex bidirectional cross-talk with other components of the neurovascular unit (NVU). Astrocytes and pericytes release cell secretomes [e.g., transforming growth factor (TGF)-β, Shh, Ang-1, Wnt] that get entrapped on the BM. The cell membrane of the endothelial cells (ECs) expresses a number of receptors for these released factors to bind and stimulate important cell signalling events that could lead to the upregulation of the tight junction (TJ) protein expressions. The BM components can also bind to their corresponding receptors expressed by the EC membranes (e.g., laminin binding to β1 integrins and agrin binding to agrin receptors). Adapted, with permission[s22], from [101].

References

1 Abbott, N.J. *et al.* (2006) Astrocyte–endothelial interactions at the blood–brain barrier. *Nat. Rev. Neurosci.* 7, 41–53

2 Abbott, N.J. (2005) Dynamics of CNS barriers: evolution, differentiation, and modulation. *Cell. Mol. Neurobiol.* 25, 5–23

3 Cecchelli, R. *et al.* (2007) Modelling of the blood–brain barrier in drug discovery and development. *Nat. Rev. Drug Discov.* 6, 650–661

4 Aday, S. *et al*. (2016) Stem cell-based human blood–brain barrier models for drug discovery and delivery. *Trends Biotechnol.* 34, 382–393

5 Syvänen, S. *et al*. (2009) Species differences in blood-brain barrier transport of three positron emission tomography radioligands with emphasis on P-glycoprotein transport. *Drug Metab. Dispos.* 37, 635–643

6 Wilhelm, I. and Krizbai, I.A. (2014) *In vitro* models of the blood–brain barrier for the study of drug delivery to the brain. *Mol. Pharm.* 11, 1949–1963

7 Cecchelli, R. *et al.* (2014) A stable and reproducible human blood-brain barrier model derived from hematopoietic stem cells. *PLoS One* 9, e99733

8 Lippmann, E.S. *et al.* (2012) Derivation of blood–brain barrier endothelial cells from human pluripotent stem cells. *Nat. Biotechnol.* 30, 783–791

9 Griep, L. *et al.* (2013) BBB on chip: microfluidic platform to mechanically and biochemically modulate blood–brain barrier function. *Biomed. Microdev.* 15, 145–150

10 Santaguida, S. *et al*. (2006) Side by side comparison between dynamic versus static models of blood–brain barrier *in vitro*: a permeability study. *Brain Res.* 1109, 1–13

11 Naik, P. and Cucullo, L. (2012) *In vitro* blood–brain barrier models: current and perspective technologies. *J. Pharm. Sci.* 101, 1337–1354

12 Bauer, H-C. *et al.* (2014) "You shall not pass"--tight junctions of the blood brain barrier. *Front. Neurosci.* 8, 392

13 Stamatovic, S.M. *et al*. (2008) Brain endothelial cell–cell junctions: how to "open" the blood brain barrier. *Curr. Neuropharmacol.* 6, 179

14 Nitta, T. *et al.* (2003) Size-selective loosening of the blood–brain barrier in claudin-5-deficient mice. *J. Cell Biol.* 161, 653–660

15 Ohtsuki, S. *et al.* (2007) Exogenous expression of claudin-5 induces barrier properties in cultured rat brain capillary endothelial cells. *J. Cell. Physiol.* 210, 81–86

16 Wolburg, H. *et al.* (2003) Localization of claudin-3 in tight junctions of the blood–brain barrier is selectively lost during experimental autoimmune encephalomyelitis and human glioblastoma multiforme. *Acta Neuropathologica* 105, 586–592

17 Liebner, S. *et al.* (2008) Wnt/β-catenin signaling controls development of the blood–brain barrier. *J. Cell Biol.* 183, 409–417

18 Günzel, D. and Alan, S. (2013) Claudins and the modulation of tight junction permeability. *Physiol. Rev.* 93, 525–569

19 Fujita, H. *et al*. (2008) Tight junction proteins claudin-2 and-12 are critical for vitamin D-dependent Ca2+ absorption between enterocytes. *Mol. Biol. Cell* 19, 1912–1921

20 Schrade, A. *et al.* (2012) Expression and localization of claudins-3 and-12 in transformed human brain endothelium. *Fluids Barriers CNS* 9, 10.1186

21 Taddei, A. *et al*. (2008) Endothelial adherens junctions control tight junctions by VE-cadherin-mediated upregulation of claudin-5. *Nat. Cell Biol.* 10, 923–934

22 Gumbleton, M. and Audus, K.L. (2001) Progress and limitations in the use of *in vitro* cell cultures to serve as a permeability screen for the blood–brain barrier. *J. Pharm. Sci.* 90, 1681–1698

23 Smith, Q.R. and Rapoport, S.I. (1986) Cerebrovascular permeability coefficients to sodium, potassium, and chloride. *J. Neurochem.* 46, 1732–1742

24 Butt, A.M. *et al.* (1990) Electrical resistance across the blood–brain barrier in anaesthetized rats: a developmental study. *J. Physiol.* 429, 47–62

25 Reichel, A. *et al*. (2003) An overview of *in vitro* techniques for blood–brain barrier studies. In *The Blood–Brain Barrier*, pp[s23]. 307–324, Springer

26 Helms, H.C. *et al.* (2016) *In vitro* models of the blood–brain barrier: an overview of commonly used brain endothelial cell culture models and guidelines for their use. *J. Cerebral Blood Flow Metabolism* 36, 862–890

27 Wuest, D.M. *et al.* (2013) Membrane configuration optimization for a murine *in vitro* blood–brain barrier model. *J. Neurosci. Methods* 212, 211–221

28 Vandenhaute, E. *et al*. (2016) Adapting coculture *in vitro* models of the blood–brain barrier for use in cancer research: maintaining an appropriate endothelial monolayer for the assessment of transendothelial migration. *Lab. Invest.* 96, 588–598

29 Wuest, D.M. and Lee, K.H. (2012) Optimization of endothelial cell growth in a murine *in vitro* blood–brain barrier model. *Biotechnol. J.* 7, 409–417

30 Bickel, U. (2005) How to measure drug transport across the blood–brain barrier. *NeuroRx* 2, 15–26

31 Czupalla, C.J. *et al.* (2014) *In vitro* models of the blood–brain barrier. *Methods Mol. Biol.* 1135, 415–437[s24]

32 Giacomini, K.M. *et al*. (2010) Membrane transporters in drug development. *Nat. Rev. Drug Discov.* 9, 215–236

33 Wong, A.D. *et al.* (2013) The blood–brain barrier: an engineering perspective. *Front. Neuroeng.* 6, 7

34 Deli, M. (2007) Blood–brain barrier models. In *Handbook of Neurochemistry and Molecular Neurobiology: Neural Membranes and Transport*, pp. [s25]29–55, Springer

35 Janzer, R.C. and Raff, M.C. (1987) Astrocytes induce blood–brain barrier properties in endothelial cells. *Nature* 325, 253–257

36 Tao-Cheng, J-H. *et al.* (1987) Tight junctions of brain endothelium *in vitro* are enhanced by astroglia. *J. Neurosci.* 7, 3293–3299

37 Deli, M.A. *et al.* (2005) Permeability studies on *in vitro* blood–brain barrier models: physiology, pathology, and pharmacology. *Cell. Mol. Neurobiol.* 25, 59–127

38 Wolff, A. *et al.* (2015) *In vitro* blood–brain barrier models--an overview of established models and new microfluidic approaches. *J. Pharm. Sci.* 104, 2727–2746

39 Dehouck, M.P. *et al.* (1990) An easier, reproducible, and mass-production method to study the blood–brain barrier *in vitro*. *J. Neurochem.* 54, 1798–1801

40 Ruchoux, M. *et al.* (2002) Lessons from CADASIL. *Ann. N. Y. Acad. Sci.* 977, 224–231

41 Smith, M. *et al.* (2007) Primary porcine brain microvascular endothelial cells: biochemical and functional characterisation as a model for drug transport and targeting. *J. Drug Target.* 15, 253–268

42 Cantrill, C.A. *et al*. (2012) An immortalised astrocyte cell line maintains the *in vivo* phenotype of a primary porcine *in vitro* blood–brain barrier model. *Brain Res.* 1479, 17–30

43 Perriere, N. *et al.* (2005) Puromycin-based purification of rat brain capillary endothelial cell cultures. Effect on the expression of blood–brain barrier-specific properties. *J. Neurochem.* 93, 279–289

44 Malina, K.C-K. *et al.* (2009) Closing the gap between the *in-vivo* and *in-vitro* blood–brain barrier tightness. *Brain Res.* 1284, 12–21

45 Ma, S.H. *et al*. (2005) An endothelial and astrocyte co-culture model of the blood–brain barrier utilizing an ultra-thin, nanofabricated silicon nitride membrane. *Lab Chip* 5, 74–85

46 Shayan, G. *et al.* (2011) Murine *in vitro* model of the blood–brain barrier for evaluating drug transport. *Eur. J. Pharm. Sci.* 42, 148–155

47 Alvarez, J.I. *et al.* (2013) Glial influence on the blood brain barrier. *Glia* 61, 1939–1958

48 Abbott, N.J. (2002) Astrocyte–endothelial interactions and blood–brain barrier permeability *J. Anatomy* 200, 629–638

49 Rubin, L. *et al*. (1991) A cell culture model of the blood–brain barrier. *J. Cell Biol.* 115, 1725–1735

50 Wolburg, H. *et al.* (1994) Modulation of tight junction structure in blood–brain barrier endothelial cells. Effects of tissue culture, second messengers and cocultured astrocytes. *J. Cell Sci.* 107, 1347–1357

51 Bicker, J. *et al*. (2014) Blood–brain barrier models and their relevance for a successful development of CNS drug delivery systems: a review. *Eur. J. Pharm. Biopharm.* 87, 409–432

52 Daneman, R. *et al.* (2010) Pericytes are required for blood-brain barrier integrity during embryogenesis. *Nature* 468, 562–566

53 Virgintino, D. *et al.* (2007) An intimate interplay between precocious, migrating pericytes and endothelial cells governs human fetal brain angiogenesis. *Angiogenesis* 10, 35–45

54 Armulik, A. *et al.* (2011) Pericytes: developmental, physiological, and pathological perspectives, problems, and promises. *Dev. Cell* 21, 193–215

55 Vandenhaute, E. *et al*. (2011) Modelling the neurovascular unit and the blood–brain barrier with the unique function of pericytes. *Curr. Neurovasc. Res.* 8, 258–269

56 Dohgu, S. *et al*. (2005) Brain pericytes contribute to the induction and up-regulation of blood–brain barrier functions through transforming growth factor-β production. *Brain Res.* 1038, 208–215

57 Berezowski, V. *et al.* (2004) Contribution of glial cells and pericytes to the mRNA profiles of P-glycoprotein and multidrug resistance-associated proteins in an *in vitro* model of the blood–brain barrier. *Brain Res.* 1018, 1–9

58 Nakagawa, S. *et al*. (2007) Pericytes from brain microvessels strengthen the barrier integrity in primary cultures of rat brain endothelial cells. *Cell. Mol. Neurobiol.* 27, 687–694

59 Nakagawa, S. *et al*. (2009) A new blood–brain barrier model using primary rat brain endothelial cells, pericytes and astrocytes. *Neurochem. Int.* 54, 253–263

60 Wakui, S. *et al.* (2006) Localization of Ang-1,-2, Tie-2, and VEGF expression at endothelial-pericyte interdigitation in rat angiogenesis. *Lab. Invest.* 86, 1172–1184

61 Hatherell, K. *et al.* (2011) Development of a three-dimensional, all-human *in vitro* model of the blood–brain barrier using mono-, co-, and tri-cultivation Transwell models. *J. Neurosci. Methods* 199, 223–229

62 Xue, Q. *et al.* (2013) A novel brain neurovascular unit model with neurons, astrocytes and microvascular endothelial cells of rat. *Int. J. Biol. Sci.* 9, 174

63 Thanabalasundaram, G. *et al.* (2011) The impact of pericytes on the blood–brain barrier integrity depends critically on the pericyte differentiation stage. *Int. J. Biochem. Cell Biol.* 43, 1284–1293

64 Weksler, B. *et al.* (2005) Blood–brain barrier-specific properties of a human adult brain endothelial cell line. *FASEB J.* 19, 1872–1874

65 Weksler, B. *et al*. (2013) The hCMEC/D3 cell line as a model of the human blood brain barrier. *Fluids Barriers CNS* 10, 16

66 Wassmer, S.C. *et al.* (2006) Platelets potentiate brain endothelial alterations induced by *Plasmodium falciparum*. *Infect. Immun.* 74, 645–653

67 Carl, S.M. *et al.* (2010) ABC and SLC transporter expression and POT substrate characterization across the human CMEC/D3 blood−brain barrier cell line. *Mol. Pharm.* 7, 1057–1068

68 Förster, C. *et al.* (2008) Differential effects of hydrocortisone and TNFα on tight junction proteins in an *in vitro* model of the human blood–brain barrier. *J. Physiol.* 586, 1937–1949

69 Urich, E. *et al.* (2012) Transcriptional profiling of human brain endothelial cells reveals key properties crucial for predictive *in vitro* blood–brain barrier models. *PloS One* 7, e38149

70 Poller, B. *et al.* (2008) The human brain endothelial cell line hCMEC/D3 as a human blood–brain barrier model for drug transport studies. *J. Neurochem.* 107, 1358–1368

71 Prudhomme, J.G. *et al.* (1996) Studies of *Plasmodium falciparum* cytoadherence using immortalized human brain capillary endothelial cells. *Int. J. Parasitol.* 26, 647–655

72 Kusch-Poddar, M. *et al*. (2005) Evaluation of the immortalized human brain capillary endothelial cell line BB19 as a human cell culture model for the blood–brain barrier. *Brain Res.* 1064, 21–31

73 Ketabi-Kiyanvash, N. *et al.* (2007) NKIM-6, a new immortalized human brain capillary endothelial cell line with conserved endothelial characteristics. *Cell Tissue Res.* 328, 19–29

74 Kannan, R. *et al.* (2000) GSH transport in human cerebrovascular endothelial cells and human astrocytes: evidence for luminal localization of Na+-dependent GSH transport in HCEC. *Brain Res.* 852, 374–382

75 Sano, Y. *et al.* (2010) Establishment of a new conditionally immortalized human brain microvascular endothelial cell line retaining an *in vivo* blood–brain barrier function. *J. Cell. Physiol.* 225, 519–528

76 Kamiichi, A. *et al.* (2012) Establishment of a new conditionally immortalized cell line from human brain microvascular endothelial cells: a promising tool for human blood–brain barrier studies. *Brain Res.* 1488, 113–122

77 Maeda, T. *et al.* (2013) Establishment and characterization of spinal cord microvascular endothelial cell lines. *Clin. Exp. Neuroimmunol.* 4, 326–338

78 Eigenmann, D.E. *et al*. (2013) Comparative study of four immortalized human brain capillary endothelial cell lines, hCMEC/D3, hBMEC, TY10, and BB19, and optimization of culture conditions, for an *in vitro* blood–brain barrier model for drug permeability studies. *Fluids Barriers CNS* 10, 1–17

79 Lippmann, E.S. *et al*. (2014) A retinoic acid-enhanced, multicellular human blood–brain barrier model derived from stem cell sources. *Sci. Rep.* 4, 4160

80 Boyer-Di Ponio, J. *et al*. (2014) Instruction of circulating endothelial progenitors *in vitro* towards specialized blood–brain barrier and arterial phenotypes. *PloS One* 9, e84179

81 Hori, S. *et al.* (2004) A pericyte-derived angiopoietin-1 multimeric complex induces occludin gene expression in brain capillary endothelial cells through Tie-2 activation *in vitro*. *J. Neurochem.* 89, 503–513

82 Cucullo, L. *et al.* (2011) The role of shear stress in blood–brain barrier endothelial physiology. *BMC Neurosci.* 12, 40

83 Cucullo, L. *et al*. (2002) A new dynamic *in vitro* model for the multidimensional study of astrocyte–endothelial cell interactions at the blood–brain barrier. *Brain Res.* 951, 243–254

84 Cucullo, L. *et al.* (2007) Development of a humanized *in vitro* blood–brain barrier model to screen for brain penetration of antiepileptic drugs. *Epilepsia* 48, 505–516

85 Cucullo, L. *et al*. (2008) Immortalized human brain endothelial cells and flow-based vascular modeling: a marriage of convenience for rational neurovascular studies. *J. Cerebral Blood Flow Metabolism* 28, 312–328

86 Booth, R. and Kim, H. (2012) Characterization of a microfluidic *in vitro* model of the blood–brain barrier (μBBB). *Lab Chip* 12, 1784–1792

87 He, Y. *et al.* (2014) Cell-culture models of the blood–brain barrier. *Stroke* 45, 2514–2526

88 Chen, Y. and Liu, L. (2012) Modern methods for delivery of drugs across the blood–brain barrier. *Adv. Drug Deliv. Rev.* 64, 640–665

89 Burgess, A. and Hynynen, K. (2013) Noninvasive and targeted drug delivery to the brain using focused ultrasound. *ACS Chem. Neurosci.* 4, 519–526

90 Scherrmann, J-M. (2002) Drug delivery to brain via the blood–brain barrier. *Vasc. Pharmacol.* 38, 349–354

91 Gaillard, P.J. *et al.* (2012) Enhanced brain drug delivery: safely crossing the blood–brain barrier. *Drug Discov. Today: Technol.* 9, e155–160

92 Veszelka, S. *et al.* (2015) Blood–brain-barrier co-culture models to study nanoparticle penetration: focus on co-culture systems. *Acta Biologica Szegediensis* 59, 1–12

93 Zhao, S. *et al.* (2012) Monitoring the transport of polymeric micelles across MDCK cell monolayer and exploring related mechanisms. *J. Control. Release* 158, 413–423

94 Hellinger, É. *et al.* (2012) Comparison of brain capillary endothelial cell-based and epithelial (MDCK-MDR1, Caco-2, and VB-Caco-2) cell-based surrogate blood–brain barrier penetration models. *Eur. J. Pharm. Biopharm.* 82, 340–351

95 Mc Carthy, D.J. *et al*. (2015) Nanoparticles and the blood–brain barrier: advancing from *in-vitro* models towards therapeutic significance. *Pharm. Res.* 32, 1161–1185

96 Engelhardt, B. and Sorokin, L. (2009) The blood–brain and the blood–cerebrospinal fluid barriers: function and dysfunction. In *Seminars in Immunopathology* ([s26]Vol. 31), pp. 497–511, Springer

97 Sixt, M. *et al.* (2001) Endothelial cell laminin isoforms, laminins 8 and 10, play decisive roles in T cell recruitment across the blood–brain barrier in experimental autoimmune encephalomyelitis. *J. Cell Biol.* 153, 933–946

98 Lohikangas, L. *et al.* (2001) Assembly of laminin polymers is dependent on β1-integrins. *Exp. Cell Res.* 265, 135–144

99 Liddington, R.C. (2001) Mapping out the basement membrane. *Nat. Struct. Biol.* 8, 573–574

100 Baeten, K.M. and Akassoglou, K. (2011) Extracellular matrix and matrix receptors in blood–brain barrier formation and stroke. *Dev. Neurobiol.* 71, 1018–1039

101 Luissint, A-C. *et al.* (2012) Tight junctions at the blood brain barrier: physiological architecture and disease-associated dysregulation. *Fluids Barriers CNS* 9, 23

102 Rascher, G. *et al.* (2002) Extracellular matrix and the blood-brain barrier in glioblastoma multiforme: spatial segregation of tenascin and agrin. *Acta Neuropathologica* 104, 85–91

103 Wolburg, H. *et al.* (2009) Agrin, aquaporin-4, and astrocyte polarity as an important feature of the blood–brain barrier. *The Neuroscientist* 15, 180–193

104 Engelhardt, S. *et al.* (2014) Cell-specific blood–brain barrier regulation in health and disease: a focus on hypoxia. *Br. J. Pharmacol.* 171, 1210–1230

105 Roberts, J. *et al*. (2012) Perlecan and the blood–brain barrier: beneficial proteolysis. *Front. Pharmacol.* 3, 1–5

106 Osada, T. *et al.* (2011) Interendothelial claudin-5 expression depends on cerebral endothelial cell–matrix adhesion by β1-integrins. *J. Cerebral Blood Flow Metabolism* 31, 1972–1985

107 Yao, Y. *et al*. (2014) Astrocytic laminin regulates pericyte differentiation and maintains blood brain barrier integrity. *Nat. Commun.* 5, 3413

108 Paolinelli, R. *et al*. (2011) The molecular basis of the blood brain barrier differentiation and maintenance. Is it still a mystery? *Pharmacol. Res.* 63, 165–171

109 Smolich, B. *et al.* (1993) Wnt family proteins are secreted and associated with the cell surface. *Mol. Biol. Cell* 4, 1267–1275

110 Akhmetshina, A. *et al.* (2012) Activation of canonical Wnt signalling is required for TGF-β-mediated fibrosis. *Nat. Commun.* 3, 735

111 Daneman, R. *et al.* (2009) Wnt/β-catenin signaling is required for CNS, but not non-CNS, angiogenesis. *Proc. Natl. Acad. Sci. U. S. A.* 106, 641–646

112 Alvarez, J.I. *et al*. (2011) The Hedgehog pathway promotes blood–brain barrier integrity and CNS immune quiescence. *Science* 334, 1727–1731

113 Tilling, T. *et al.* (1998) Basement membrane proteins influence brain capillary endothelial barrier function *in vitro*. *J. Neurochem.* 71, 1151–1157

114 Savettieri, G. *et al.* (2000) Neurons and ECM regulate occludin localization in brain endothelial cells. *Neuroreport* 11, 1081–1084

115 Hartmann, C. *et al.* (2007) The impact of glia-derived extracellular matrices on the barrier function of cerebral endothelial cells: an *in vitro* study. *Exp. Cell Res.* 313, 1318–1325

116 Levy, A.F. *et al.* (2014) Influence of basement membrane proteins and endothelial cell-derived factors on the morphology of human fetal-derived astrocytes in 2D. *PloS One* 9, e92165

117 Placone, A.L. *et al.* (2015) Human astrocytes develop physiological morphology and remain quiescent in a novel 3D matrix. *Biomaterials* 42, 134–143

118 East, E. *et al.* (2009) A versatile 3D culture model facilitates monitoring of astrocytes undergoing reactive gliosis. *J. Tissue Eng. Regen. Med.* 3, 634–646

119 Paramonov, S.E. *et al.* (2006) Self-assembly of peptide-amphiphile nanofibers: the roles of hydrogen bonding and amphiphilic packing. *J. Am. Chem. Soc.* 128, 7291–7298

120 Mendes, A.C. *et al.* (2013) Self-assembly in nature: using the principles of nature to create complex nanobiomaterials. *Wiley Interdiscip. Rev. Nanomed. Nanobiotechnol.* 5, 582–612

121 Dankers, P.Y. *et al*. (2011) Bioengineering of living renal membranes consisting of hierarchical, bioactive supramolecular meshes and human tubular cells. *Biomaterials* 32, 723–733

122 Ferreira, D.S. *et al.* (2015) Molecularly engineered self-assembling membranes for cell-mediated degradation. *Adv. Healthcare Mater.* 4, 602–612

123 Gosselet, F. *et al*. (2013) Amyloid-β peptides, Alzheimer's disease and the blood–brain barrier. *Curr. Alzheimer Res.* 10, 1015–1033

124 Ge, S. *et al.* (2005) Where is the blood–brain barrier… really? *J. Neurosci. Res.* 79, 421–427

125 Kuo, Y-C. and Shih-Huang, C-Y. (2013) Solid lipid nanoparticles carrying chemotherapeutic drug across the blood–brain barrier through insulin receptor-mediated pathway. *J. Drug Target.* 21, 730–738

126 Kuo, Y-C. and Ko, H-F. (2013) Targeting delivery of saquinavir to the brain using 83-14 monoclonal antibody-grafted solid lipid nanoparticles. *Biomaterials* 34, 4818–4830

127 Pilakka-Kanthikeel, S. *et al.* (2013) Targeted brain derived neurotropic factors (BDNF) delivery across the blood–brain barrier for neuro-protection using magnetic nano carriers: an *in-vitro* study. *PLoS One* 8, e62241

128 Fenart, L. *et al*. (1999) Evaluation of effect of charge and lipid coating on ability of 60-nm nanoparticles to cross an in vitro model of the blood–brain barrier. *J. Pharmacol. Exp. Ther.* 291, 1017–1022

129 Lu, W. *et al.* (2005) Cationic albumin-conjugated pegylated nanoparticles as novel drug carrier for brain delivery. *J. Control. Release* 107, 428–448

130 Liu, Y. *et al.* (2010) A leptin derived 30-amino-acid peptide modified pegylated poly-L-lysine dendrigraft for brain targeted gene delivery. *Biomaterials* 31, 5246–5257

131 Kreuter, J. *et al.* (2003) Direct evidence that polysorbate-80-coated poly (butylcyanoacrylate) nanoparticles deliver drugs to the CNS via specific mechanisms requiring prior binding of drug to the nanoparticles. *Pharm. Res.* 20, 409–416

132 Kuo, Y-C. and Chung, C-Y. (2012) Transcytosis of CRM197-grafted polybutylcyanoacrylate nanoparticles for delivering zidovudine across human brain-microvascular endothelial cells. *Colloids Surf. B Biointerfaces* 91, 242–249

133 Chaturvedi, M. *et al.* (2014) Tissue inhibitor of matrix metalloproteinases-1 loaded poly (lactic-co-glycolic acid) nanoparticles for delivery across the blood–brain barrier. *Int. J. Nanomed.* 9, 575

134 Kuo, Y-C. and Lee, C-L. (2012) Methylmethacrylate–sulfopropylmethacrylate nanoparticles with surface RMP-7 for targeting delivery of antiretroviral drugs across the blood–brain barrier. *Colloids Surf. B Biointerfaces* 90, 75–82

135 Chen, Y-C. *et al.* (2013) Effects of surface modification of PLGA-PEG-PLGA nanoparticles on loperamide delivery efficiency across the blood–brain barrier. *J. Biomater. Appl.* 27, 909–922

[s27]

136 Gao, H. *et al.* (2014) Study and evaluation of mechanisms of dual targeting drug delivery system with tumor microenvironment assays compared with normal assays. *Acta Biomaterialia* 10, 858–867

137 Meister, S. *et al*. (2013) Nanoparticulate flurbiprofen reduces amyloid-beta42 generation in an *in vitro* blood–brain barrier model. *Alzheimers Res. Ther.* 5, 51

138 Wagner, S. *et al.* (2010) Nanoparticulate transport of oximes over an *in vitro* blood–brain barrier model. *PLoS One* 5, e14213

139 Bonoiu, A. *et al*. (2009) MMP-9 gene silencing by a quantum dot–siRNA nanoplex delivery to maintain the integrity of the blood brain barrier. *Brain Res.* 1282, 142–155

140 Tian, X. *et al.* (2015) LRP-1-mediated intracellular antibody delivery to the central nervous system. *Sci. Rep.* 5, 11990

141 Xie, Y. *et al.* (2005) Transport of nerve growth factor encapsulated into liposomes across the blood–brain barrier: *in vitro* and *in vivo* studies. *J. Control. Release* 105, 106–119

142 Re, F. *et al.* (2011) Functionalization of liposomes with ApoE-derived peptides at different density affects cellular uptake and drug transport across a blood–brain barrier model. *Nanomed. Nanotechnol. Biol. Med.* 7, 551–559

143 Huang, F-Y.J. *et al*. (2013) *In vitro* and *in vivo* evaluation of lactoferrin-conjugated liposomes as a novel carrier to improve the brain delivery. *Int. J. Mol. Sci.* 14, 2862–2874

144 Ying, X. *et al.* (2010) Dual-targeting daunorubicin liposomes improve the therapeutic efficacy of brain glioma in animals. *J. Control. Release* 141, 183–192

145 Teow, H.M. *et al.* (2013) Delivery of paclitaxel across cellular barriers using a dendrimer-based nanocarrier. *Int. J. Pharm.* 441, 701–711

146 Li, Y. *et al*. (2012) A dual-targeting nanocarrier based on poly (amidoamine) dendrimers conjugated with transferrin and tamoxifen for treating brain gliomas. *Biomaterials* 33, 3899–3908

147 Xie, Y-T. *et al*. (2012) Brain-targeting study of stearic acid-grafted chitosan micelle drug-delivery system. *Int. J. Nanomed.* 7, 3235–3244

148 Hornok, V. *et al*. (2012) Preparation and properties of nanoscale containers for biomedical application in drug delivery: preliminary studies with kynurenic acid. *J. Neural Transm.* 119, 115–121

149 Dakwar, G.R. *et al.* (2012) Delivery of proteins to the brain by bolaamphiphilic nano-sized vesicles. *J. Control. Release* 160, 315–321

150 Banks, W.A. (2016) From blood–brain barrier to blood–brain interface: new opportunities for CNS drug delivery. *Nat. Rev. Drug Discov.* 15, 275–292

151 Mouw, J.K. *et al.* (2014) Extracellular matrix assembly: a multiscale deconstruction. *Nat. Rev. Mol. Cell Biol.* 15, 771–785

152 Durbeej, M. (2010) Laminins. *Cell. Tissue Res.* 339, 259–268

153 Kalluri, R. (2003) Basement membranes: structure, assembly and role in tumour angiogenesis. *Nat. Rev. Cancer* 3, 422–433

154 Bezakova, G. and Ruegg, M.A. (2003) New insights into the roles of agrin. *Nat. Rev. Mol. Cell Biol.* 4, 295–309

155 Hohenester, E. and Yurchenco, P.D. (2013) Laminins in basement membrane assembly. *Cell Adh. Migr.* 7, 56–63

Jayati Banerjee

Jayati Banerjee received a PhD in pharmaceutical sciences from North Dakota State University, USA. Thereafter, Jayati worked as a postdoctoral research fellow in peptide drug discovery and development at Torrey Pines Institute for Molecular Studies in Florida, USA. In 2015, Jayati joined Queen Mary University of London as a Marie Curie postdoctoral fellow to pursue research on developing higher-order self-supporting supramolecular hydrogels through self-assembly of simple building blocks such as polysaccharides and peptides for applications in tissue engineering and regenerative medicine.

Yejiao Shi

Yejiao Shi received her BS in pharmaceutics from China Pharmaceutical University and is currently a PhD candidate supervised by Dr Helena Azevedo under the medical engineering programme at Queen Mary, University of London. Her research is focused on developing an intracellular delivery system based on the self-assembled micelles of cell-penetrating peptide amphiphiles.

Helena S. Azevedo

Dr Helena S. Azevedo obtained an MEng degree in biological engineering from the University of Minho (Portugal) and her PhD from De Montfort University (UK). She completed post-doctoral work with Professor Reis at the 3B's Research Group at the University of Minho working on biomaterials for applications in drug delivery and tissue engineering. Before becoming an independent researcher at the University of Minho, she was a Marie Curie fellow in Chicago with Professor Stupp at Northwestern University where she developed work on self-assembling biomaterials using peptide amphiphiles. Currently, she is a Senior Lecturer in biomedical engineering and biomaterials in the School of Engineering & Materials Science at Queen Mary University of London (QMUL) and the Director of Operations of the Institute of Bioengineering also at QMUL. Her research interests include the use of bottom-up approaches to develop biomimetic matrices for *in vitro* cell culture platforms to better understand the role of matrix signals in directing cellular processes.

Table 1. Commonly used *in vitro* BBB models for studying uptake and delivery of nanoformulations into the brain; different types of nanoparticle are acting as carriers for loaded cargoes, which can include chemotherapeutics, diagnostics, fluorescent dyes serving as model drugs, genes, proteins and antibodies

Loaded therapeutics or cargoes	Type of nanocarrier	Ligand used for surface modification	Nature of BECs	Co-culture cell type	Observations	Refs
Carmustine (chemotherapeutics)	Solid lipid NP	83-14 mAb; targets insulin receptor	Primary human	Human astroglia	Enhanced permeability and cellular uptake of carmustine via insulin receptor mediated endocytosis	[125]
Saquinavir (antiretroviral)	Solid lipid NP	83-14 mAb; targets insulin receptor	Primary human	Human astroglia	BBB permeability increases with increasing concentrations of mAb. The enhanced permeability is the result of recognition and stimulation of cell surface insulin receptors by mAb	[126]
BDNF	Magnetic iron oxide NP	None	Primary human	Human astroglia	Nearly 73% of BDNF bound magnetically guided NP were able to cross the BBB	[127]
Albumin (model for protein)	Maltodextran	Cationic charge lipid coating on the surface	Primary bovine	Rat glia	Increased permeability of albumin	[128]
6-Coumarin (fluorescent probe)	PEG-PLA NP	Cationic BSA	Primary rat	Rat astrocytes	Significant accumulation of cationic NPs in the lateral, third and the peri ventricles	[129]
DNA (gene delivery)	DGL-PEG NP	Leptin derived 30 amino acid peptide (Leptin 30)	b.End3 cell line, mouse	None	The polymer was effectively transported across the BBB	[130]
Dalargin an endorphin; opioid analgesic	PBCA NP	Polysorbate-80 coating	Primary bovine	Rat glia	Not given	[131]
Zidovudine (retroviral)	PBCA NP	CRM197 (targets diphtheria toxin	Primary human	Human astroglia	Enhanced permeability of zidovudine with increasing CRM-197 concentration in the formulation	[132]

		receptor)				
TIMP-I (example of protein delivery)	PLGA NP	Polysorbate-80 coating	Primary rat and RBE4 cell line, rat	None	About 11.21 ±1.35% of TIMP-I was able to cross the EC monolayer whereas only TIMP-1 and TIMP-1-PLGA (without polysorbate) were not able to penetrate the cultured monolayer	[133]
D4T, delavirdine and saquinavir (antiretroviral drugs)	MMSM NP	Bradykinin type II receptor agonist (RMP-7)	Primary human	Human astroglia	RMP-7 enhanced the paracellular and transcellular permeability of the three drugs across the EC monolayer and the order of increase of P_e (D4T>saquinavir>delavirdine)	[134]
Loperamide (analgesic)	PLGA-PEG-PLGA NP	Polxamer 188 or polysorbate 80 coating	RBE4 cell line, rat	Rat C6	BBB permeability of drug encapsulated NP was 13.7-fold higher than free drug solution	[135]
Docetaxel (anticancer activity)	PEG-PCL NP	AS1411 aptamer for glioma targeting and TGN peptide for BBB targeting	b.End3 cell line, mouse	Rat C6	Demonstrated improved penetration power through b.End3 and C6 spheroids with significant decrease in growth of tumour spheroid	[136]
Flubiprofen (therapeutics for Alzheimer's disease)	PLA NP	None	b.End3, mouse	None	PLA-flubiprofen was able to penetrate the BBB and the transported flubiprofen could modulate the activity of enzyme Y-secretase	[137]
Oximes (muscarinic receptor antagonist)	PEG-HSA NP	ApoE (targets LDL receptors on brain ECs)	Primary porcine	None	Higher concentration of Apo-E modified oxime bound nanoparticle was detected in basolateral compartment compared with controls	[138]
siRNA for MMP-9 gene silencing	Quantum dots	None	Primary human	Human astroglia	Increased uptake and MMP-9 gene silencing	[139]
IgG (model antibody)	Polymersomes (synthetic vesicles formed by amphiphilic co-polymers)	Angiopep-2 and rabies virus glycoprotein peptide receptor target: LRP-1	bEnd.3, mouse	Mouse pericyte or C8-D1A mouse astrocytic cell line	Not given	[140]
NGF (model for GF	Liposomes	RMP-7; ligand	Primary	None	P_e of nanoparticle formulation containing NGF =	[141]

delivery)		for B2 receptor on BMECs	mouse		2.58 ±0.11 × 10^6 cm s^{-1} (P_e for free NGF = 1.85 ±0.04 × 10^6 cm·s^{-1})	
Curcumin derivative (natural component of spices such as turmeric, believed to possess anti-inflammatory properties)	Nanoliposome	ApoE-derived peptide	RBE4 cell line, rat	None	The P_e value of curcumin was enhanced with increasing loading density of ApoE peptide	[142]
^{99m}Tc-BMEDA serving as diagnostic	PEGylated liposomes	Lactoferrin	b.End3, mouse	None	Enhanced uptake by the cells; amount uptake remained unaffected by incubation time	[143]
Daunorubicin (anticancer activity)	Sugar and transferrin coated dual targeting liposome	Transferrin	Primary murine	Murine C6 glioma cell line	The transport ratio across the EC monolayer of daunorubicin in liposomal formulation was 24.9% compared with 3.1% of free drug	[144]
Paclitaxel (anticancer activity)	Third generation G3 PAMAM dendrimer	None	Primary porcine	None	The dendrimer–drug conjugates exhibited increased P_{app} in either directions across the transwell culture of EC compared with unmodified dendrimer and free drug	[145]
7 Doxorubicin (anticancer activity)	4th generation PAMAM dendrimer conjugated with transferrin and tamoxifen	pH sensitive transferrin tamoxifen acting as P-gp inhibitor	Primary murine	Murine C6 glioma	The drug formulation showed a transport ratio of 6% in 3 h and the carrier was internalised by C6 glioma cells after transport across the cultured EC monolayer	[146]
Doxorubicin (anticancer activity)	Stearic acid grafted chitosan micelle	None	b.End3, mouse	Mouse C6 glioma	Enhanced uptake of the micelles by b.End3 cells. Cytoxicity of doxorubicin micelle towards C6 glioma cells was 2.664 ±0.036 µg/ml verses 0.181 ±0.066 µg/ml of free drug	[147]
Kynurenic acid (endogenous glutamate antagonist)	Triton™ X 100 and Lutensol® AP 20 micelles	None	Primary rat	Rat astrocytes	BBB permeability was significantly higher for encapsulated kynurenic acid compared to the free acid	[148]
BSA-FITC (fluorescent	Bolaamphiphilic	Acetylcholine	b.End3,	None	Higher cellular uptake of BSA-FITC encapsulated	[149]

labelled protein for detection)	nano-sized cationic vesicles	surface bound	mouse		bolaamphiphiles compared with free BSA-FITC at 37°C	

Abbreviations: ApoE, apoliprotein E; BBB, blood–brain barrier; BDNF, brain-derived neurotrophic factor; BEC, brain endothelial cells; BMEDA, *N*,*N*-bis(2-mercaptoethyl-N′,N′diethylethylene diamine); CRM-197, ligand for diphtheria toxin receptor; DGL, dendrigraft poly-L-lysine; FITC, fluorescein isothiocyanate; HAS, human serum albumin; IgG, immunoglobulin G; LDL, low-density lipoprotein; mAb, monoclonal antibody; MMSM, methyl-methacrylate-sulphopropyl-methaacrylate; MMP-9, matrix metalloproteinase-9; NGF, nerve growth factor; NP, nanoparticle; PAMAM, polyamidoamine; P_{app}, apparent permeability coefficient; PBCA, poly-butylcyanoacrylate; PEG, polyethylene glycol; PLA, poly-lactic acid; PLGA, poly-lactic-co-glycolic acid; PLA, poly-L-lactide; RMP-7, receptor-mediated permeabiliser-7; TIMP-I, tissue inhibitor of matrix metalloproteinase-I; cereport, a bradykinin analogue.

Table 2. Summary of advantages and limitations of *in vitro* cell-based BBB models

***In vitro* BBB models**	**Pros**	**Cons**
Transwell monoculture model 2D culture of BEC monolayers under static conditions (Figure 3a)	• Simple and cost-effective • Can be cultured with astrocyte-conditioned media • Highly convenient for high-throughput screens	• Fast de-differentiation of endothelial monolayers leading to loss in phenotype and functions • Influence of neighbouring NVU components (astrocytes, pericytes and neurons) on endothelial cell differentiation is absent • Inadequate paracellular barrier tightness
Transwell co-culture model (static model) 2D culture of EC monolayers in presence of either astrocytes or pericytes (Figure 3). Two types of orientation are possible: (i) contact (back-to-back) with astrocytes or pericytes (Figure 3bii,3biv) and (ii) non-contact (non back-to-back) (Figure 3bi,3biii)	• Enhanced barrier tightness and less EC de-differentiation in comparison with monoculture models • The influence of astrocytes or pericytes on barrier functions can be evaluated	• More complex than monoculture models • Variation in research results • Astrocyte phenotypic morphology is often not described or astrocytes might even adopt a rounded morphology instead of usual star-shaped with protrusions and branches • The thickness of the semipermeable membrane insert does not accurately reflect the true thickness of the BM *in vivo*, which is comparatively much thinner
Transwell tri-culture model (static model) Culture of ECs in presence of astrocytes and pericytes or astrocytes and neurons. Contact and non-contact formats are possible (Figs 3ci—3civ)	• Resembles more closely the actual *in vivo* brain anatomy • Some of the reported models show considerable improvement in BBB phenotype and paracellular permeability than co-culture models	• Complex to set up • Lack of reproducibility and variation in data • Astrocyte morphology not described categorically • Inclusion of pericytes in some models did not improve barrier properties • Access to three different cell types is required
Static tri-culture models using EC derived from stem cells (pluripotent or hematopoietic)	• Excellent source for establishing human *in vitro* BBB models • Scalable; can be produced at large scales • High TEER more close to *in vivo* parameter using pluripotent human stem cells	• Differentiation process is complex • Decrease in TEER within short time intervals
Dynamic *in vitro* BBB models (Figure 4)	• Considers the effect of *in vivo* sheer stress • Improved TEER compared with static models	• Require higher cell numbers • Maintenance of high flow rate owing to large volume of the hollow tubes

	• Design allows co-culture with astrocytes	• Technically challenging • Incompatible with high-throughput screening
Microfluidic models	• Requires less cell number • Can consider the effect of sheer stress • Improvement in paracellular barrier functions • Visualisation of cells is possible	• The exact geometry of the BMEC phenotype is not very well defined • TEER values are moderate
Hypothetical model using bioactive synthetic BM	• Considers the realistic effect of brain microenvironment • Can mimic the supramolecular architecture of the natural BM • Ability to regulate cell phenotypes by providing biochemical cues within the synthetic BM • Fixed composition leading to improvement in reproducibility of results • Possibility of customisation for performing mechanistic studies • Can be endowed with the ability to entrap and release soluble factors in a controlled manner • Ability to re-establish any of the models on this new cell culture platform • Control thickness of synthetic BM	• Challenges are there to design and fabricate artificial membranes • Requires knowledge on molecular engineering of biomaterials • Has to support the culture of cells of the NVU • Will require rigorous optimisation owing to scarcity of previous literature reports

Abbreviations: BBB, blood–brain barrier;

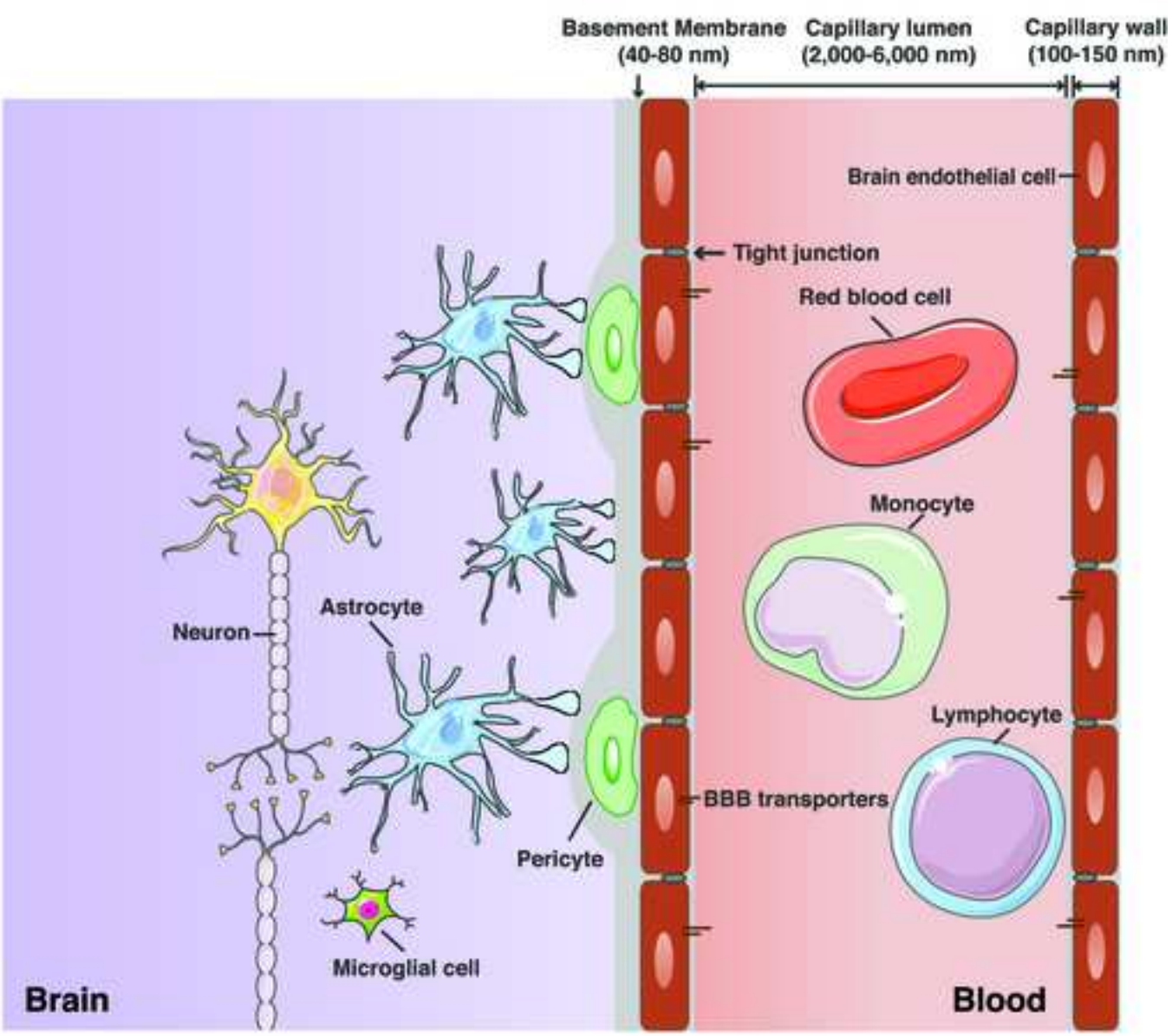

Figure 2

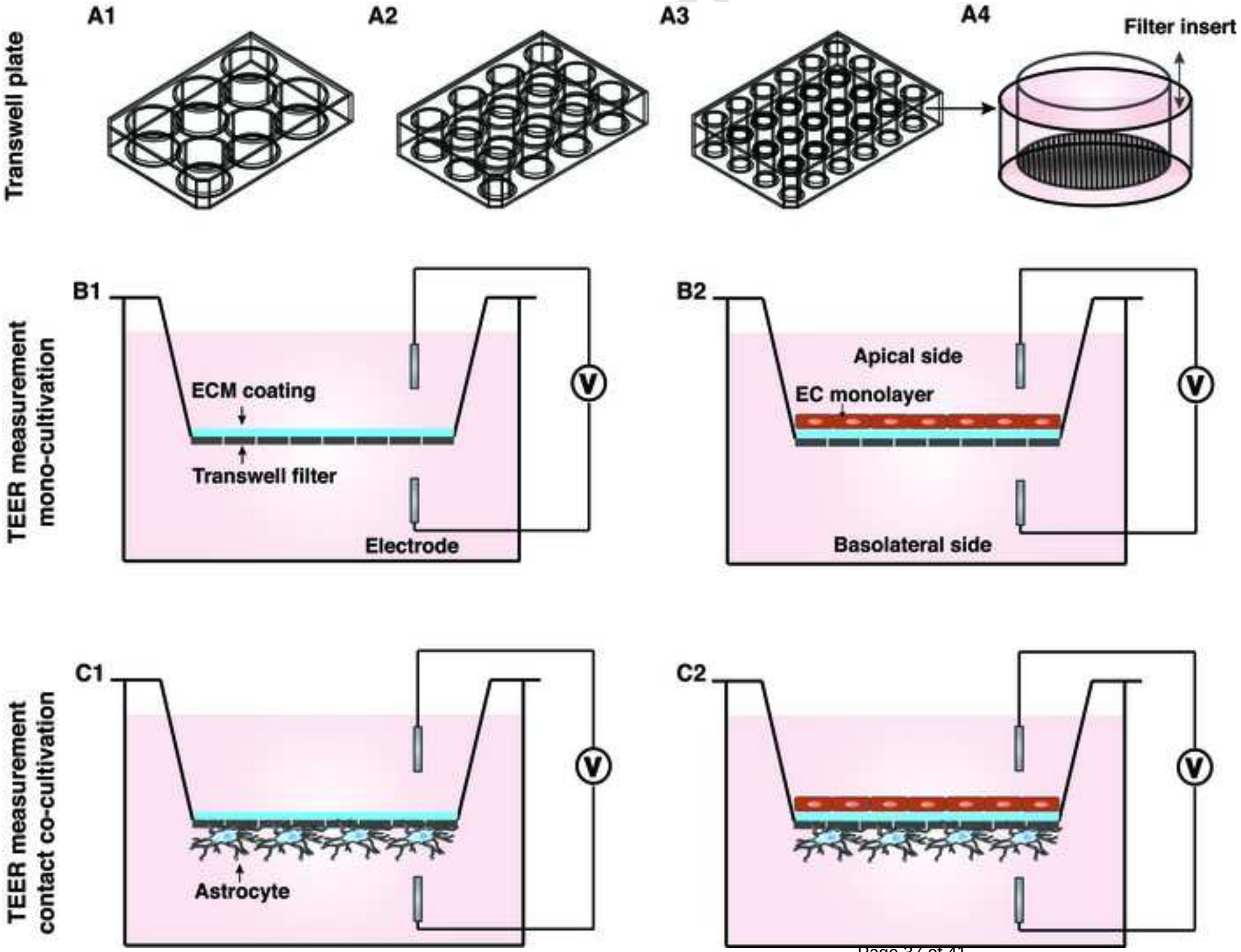
Transwell plate
A1
A2
A3
A4
Filter insert
TEER measurement mono-cultivation
B1
ECM coating
Transwell filter
Electrode
B2
Apical side
EC monolayer
Basolateral side
TEER measurement contact co-cultivation
C1
Astrocyte
C2

Figure 3

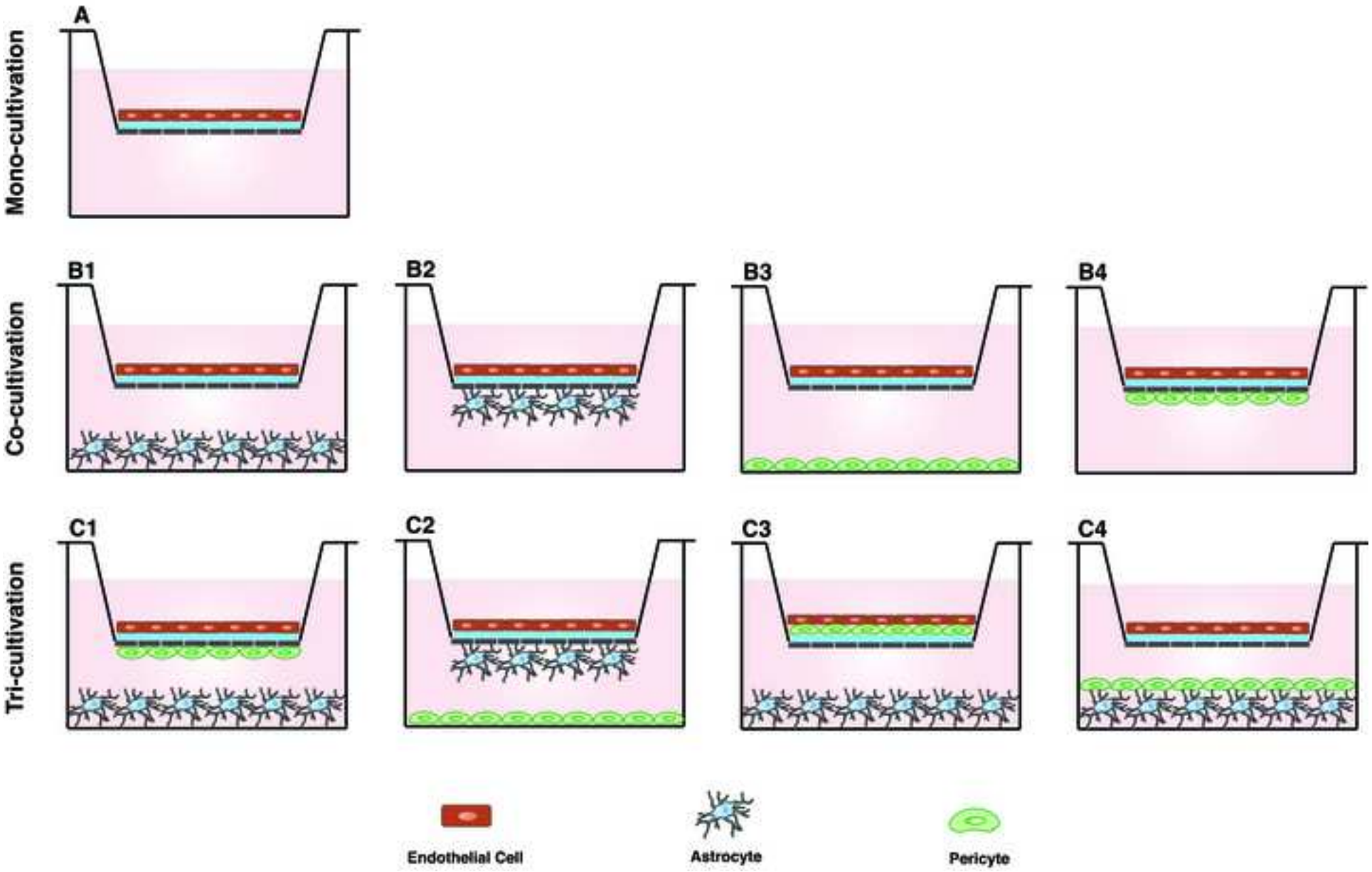
Mono-cultivation
A
Co-cultivation
B1
B2
B3
B4
Tri-cultivation
C1
C2
C3
C4
Endothelial Cell
Astrocyte
Pericyte

Figure 4

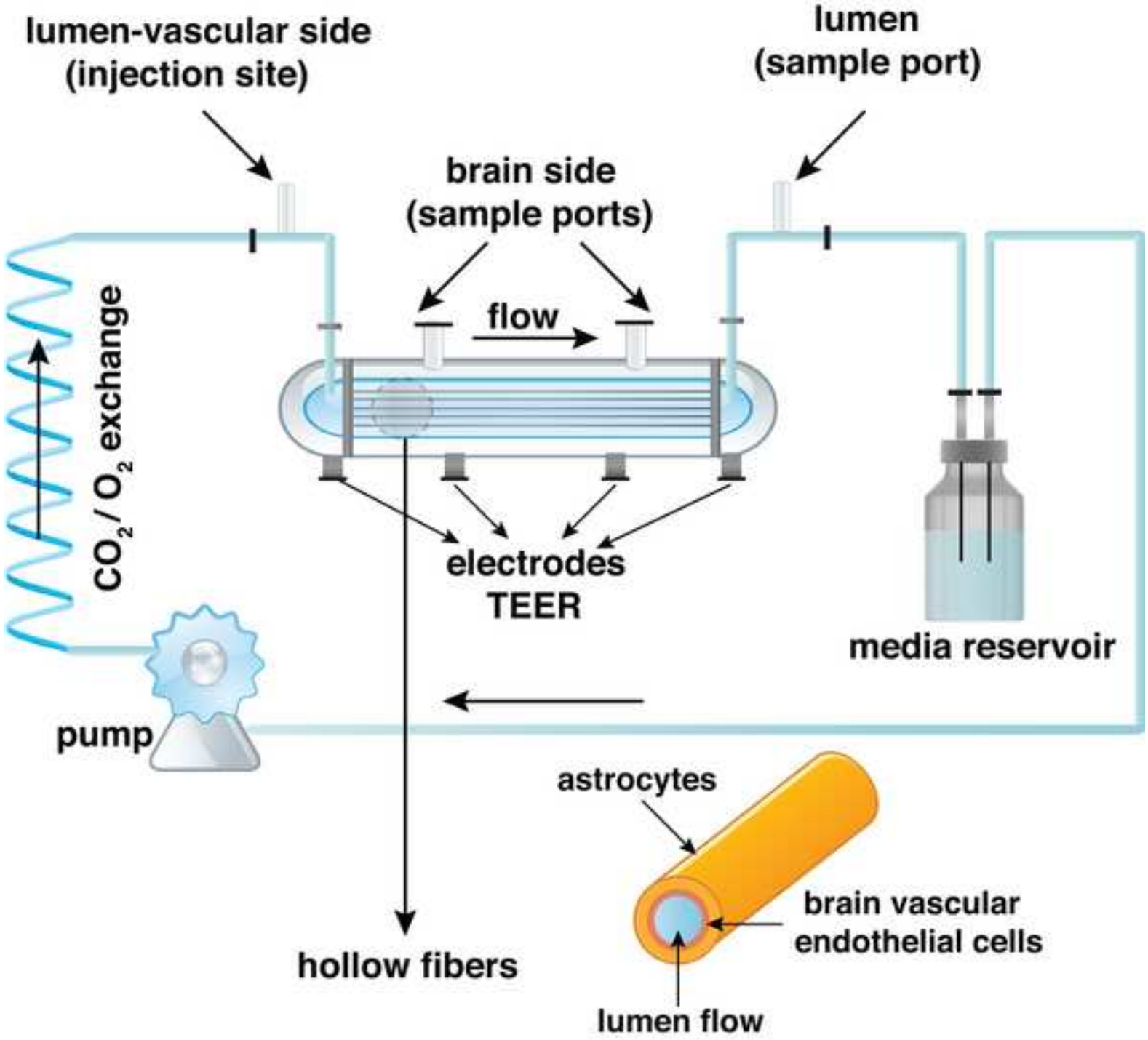
lumen-vascular side
(injection site)
lumen
(sample port)
brain side
(sample ports)
flow
CO_2 / O_2 exchange
electrodes
TEER
media reservoir
pump
astrocytes
brain vascular
endothelial cells
hollow fibers
lumen flow

Figure 5

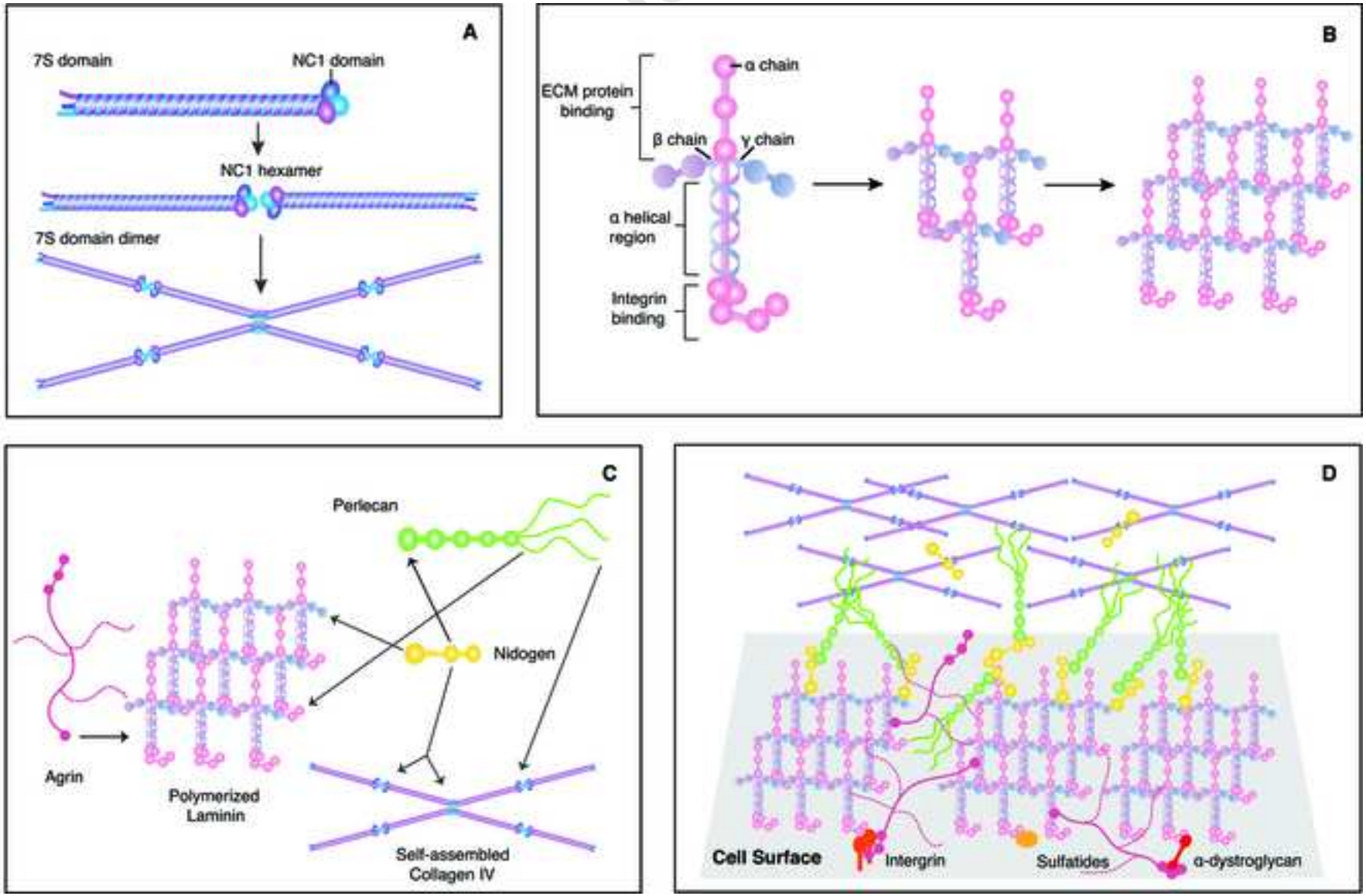
A
7S domain
NC1 domain
NC1 hexamer
7S domain dimer
B
ECM protein binding
α chain
β chain
γ chain
α helical region
Integrin binding
C
Perlecan
Nidogen
Agrin
Polymerized Laminin
Self-assembled Collagen IV
D
Cell Surface
Integrin
Sulfatides
α-dystroglycan

Figure 6

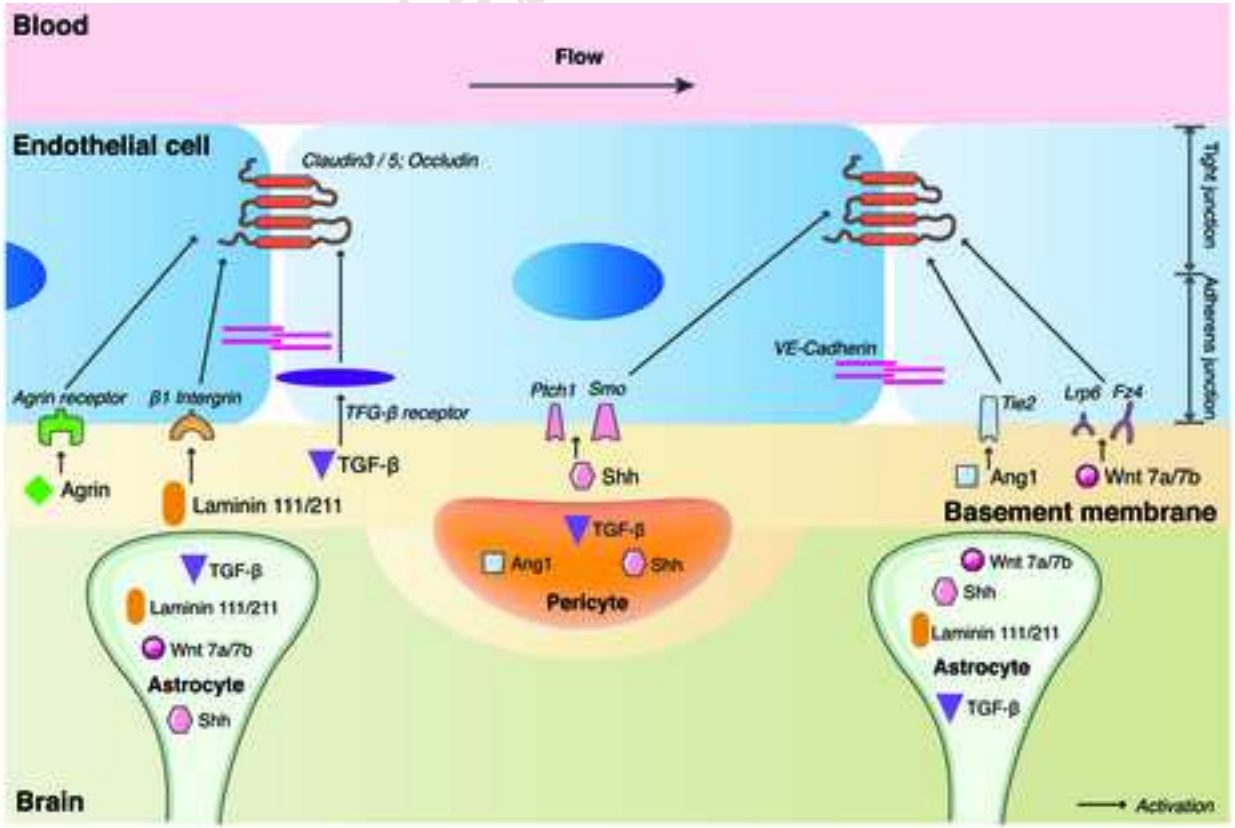
Blood
Flow
Endothelial cell
Claudin3 / 5; Occludin
Tight junction
Adherens junction
VE-Cadherin
Agrin receptor
β1 Integrin
TFG-β receptor
Ptch1
Smo
Tie2
Lrp6
Fz4
Agrin
Laminin 111/211
TGF-β
Shh
Ang1
Wnt 7a/7b
Basement membrane
TGF-β
Ang1
Shh
Pericyte
TGF-β
Laminin 111/211
Wnt 7a/7b
Astrocyte
Shh
Wnt 7a/7b
Shh
Laminin 111/211
Astrocyte
TGF-β
Brain
Activation